# Nonlinear dynamics of coupled oscillators in 1:2 internal resonance: effects of the non-resonant quadratic terms and recovery of the saturation effect

**Zein Alabidin Shami · Yichang Shen · Christophe Giraud-Audine · Cyril Touzé · Olivier Thomas**

**Abstract** This article considers the nonlinear dynamics of coupled oscillators featuring strong coupling in 1:2 internal resonance. In forced oscillations, this particular interaction is the source of energy exchange, leading to a particular shape of the response curves, as well as quasi-periodic responses and a saturation phenomenon. These main features are embedded in the simplest system which considers only the two resonant quadratic monomials conveying the 1:2 internal resonance, since they are the proeminent source allowing one to explain these phenomena. However, it has been shown recently that those features can be substantially modified by the presence of non-resonant quadratic terms. The aim of the present study is thus to explain the effect of the non-resonant quadratic terms on the dynamics. To that purpose, the normal form up to the third order is used, since the effect of the non-resonant quadratic terms will be transferred into the resonant cubic terms. Analytical solutions are detailed using a second-order mutliple scale expansion. A thorough investigation of the backbone curves, their stability and bifurcation, and the link to the forced–damped solutions, is detailed, showing in particular interesting features that had not been addressed in earlier studies. Finally, the saturation effect is investigated, and it is shown how to correct the detuning effect of the cubic terms thanks to a specific tuning of non-resonant quadratic terms and resonant cubic terms. This choice, derived analytically, is shown to extend the validity of the saturation effect to larger amplitudes, which can thus be used in all applications where this effect is needed e.g. for control.

**Keywords** Nonlinear modes · Backbone curves · Forced response · Invariant manifolds · Quadratic coupling · Normal form · Saturation phenomenon · Second order multiple scale expansion

Z. A. Shami (✉) · O. Thomas
Arts et Métiers Institute of Technology, LISPEN, HESAM Université, 59000 Lille, France
e-mail: zein_alabidin.shami@ensam.eu

O. Thomas
e-mail: olivier.thomas@ensam.eu

Y. Shen · C. Touzé
IMSIA, ENSTA Paris, CNRS, EDF, CEA, Institut Polytechnique de Paris, 828 Boulevard des Maréchaux, 91762 Palaiseau Cedex, France
e-mail: yichang.shen@ensta-paris.fr

C. Touzé
e-mail: cyril.touze@ensta-paris.fr

C. Giraud-Audine
Arts et Métiers Institute of Technology, L2EP, HESAM Université, 59000 Lille, France
e-mail: christophe.giraud-audine@ensam.eu

## 1 Introduction

The vibratory behaviour of nonlinear systems can be very complex as compared to linear ones, showing,

in particular, a dependence of its characteristic frequencies upon the amplitude, bifurcations associated to stable and unstable solutions, periodic response with rich harmonics content as well as more complex quasi-periodic and chaotic responses [1–3]. Those phenomena are often related to strong nonlinear couplings between the degrees of freedom (DOFs) of the system, leading to energy exchanges between them. Important couplings are generally fostered by particular relationships between the characteristic frequencies, leading to the important concept of internal resonance (IR) in vibration theory [4]; but other kind of couplings might also appear for systems with widely spaced frequencies [5].

The specific case of a 1:2 internal resonance is met when two nonlinear oscillators have their eigen-frequencies $\omega_1$ and $\omega_2$ such that $\omega_2 \simeq 2\omega_1$. This case has been the subject of numerous studies in the past, see e.g. [1, 4, 6–9]. In general, the 1:2 case is studied by considering only the quadratic terms and more specifically the two resonant monomials that are responsible of the strong coupling between the two oscillators, see e.g. [1, 10] for the simplified equations (normal form) to use for such case, as well as [11, 12] for general discussion on the normal form and the resonant monomials. The dynamics of such quadratically coupled nonlinear oscillators display a rich behaviour with two families of backbone curves [10, 13], appearance of quasi-periodic behaviour [1], and analytic expression of the locus of Neimark–Sacker bifurcation [10].

A particularly interesting feature of systems with 1:2 internal resonance is the saturation effect that is observed in the forced response, when the external excitation frequency $\Omega$ is in the vicinity of the second mode: $\Omega \simeq \omega_2$. As shown for example in [1], once the coupling is effective, then the amplitude of the second mode stays constant for increasing forcing amplitude, while the amplitude of the first mode (not excited by the load) increases, meaning that all the energy, input to the second oscillator, is transferred to the first. This saturation effect is important and can be used with the purpose of controlling the amplitude of the second mode, enforcing its saturation to a maximum amplitude. Successful applications have been reported for example in [14–16].

Recently, it has been shown both theoretically and experimentally in [17, 18] that the non-resonant quadratic terms play an important role in the saturation effect if one goes to moderately large amplitude. Consequently, a fine tuning of a vibration absorber based on the saturation effect needs to properly address not only the resonant quadratic terms, but also the non-resonant ones, in order to obtain a comfortable range of amplitude where the saturation effect is effective. The aim of this paper is to reconsider theoretically the effect of these non-resonant quadratic terms on the dynamics of the system with 1:2 internal resonance, in order to extend the amplitude range of the saturation effect.

Numerous analytical methods have been proposed in the past in order to derive approximate solutions to nonlinear vibration problems thanks to asymptotic expansions. In this realm, the normal form approach is particularly appealing since it conveys very important meaning related to nonlinear resonances [11, 12, 19, 20], derives the simplest form of the dynamics, and expresses its skeleton [21, 22]. It can also be used for model order reduction, see e.g. [23–25], and has a strong relationship with the parametrisation method of invariant manifold, see e.g. [26, 27], such that the normal form dictates the reduced dynamics on an invariant manifold and can be used for building ex-nihilo models [11]. In this contribution, the normal form is used to analyze the dynamics of the system with 1:2 internal resonance. Interestingly, whereas general formulations for deriving real normal forms of coupled oscillators are derived in [11, 23], they are restricted to the case without internal resonance. The computation of the normal form, up to the cubic term, with a 1:2 internal resonance, needs thus a particular development. A first aim of this paper is thus to make this derivation and gives the expression of the normal form with 1:2 resonance up to cubic order.

The second aim of the paper is to analyze the nonlinear dynamics of the system with 1:2 internal resonance up to cubic terms. Recent studies derived important results about the topology of the solutions in the unforced conservative case (nonlinear modes/backbone curves) [10, 13]. These results will be here enlarged to the next order by analyzing the effects of the cubic terms. In the normal form derivation, the non-resonant quadratic coefficients are reported to the cubic order, in the trivially resonant terms. Hence, their effect can be tracked and analyzed. The last aim of the study is thus to show how the non-resonant quadratic terms have important effects on the nonlinear dynamics and more particularly on the saturation

effect. At last, it is shown analytically how to tune non-resonant quadratic terms and resonant cubic ones, in order to extend the amplitude validity region where the saturation effect is particularly efficient.

## 2 Equations of motion, normal form and multiple scales solution

The starting point is a conservative two DOFs system with smooth nonlinearities, in the form of a Taylor expansion up to the third order:

$$\ddot{X}_1 + \omega_1^2 X_1 + g_{11}^1 X_1^2 + g_{12}^1 X_1 X_2 + g_{22}^1 X_2^2 + h_{111}^1 X_1^3 + h_{112}^1 X_1^2 X_2 + h_{122}^1 X_1 X_2^2 + h_{222}^1 X_2^3 = 0, \tag{1a}$$

$$\ddot{X}_2 + \omega_2^2 X_2 + g_{11}^2 X_1^2 + g_{12}^2 X_1 X_2 + g_{22}^2 X_2^2 + h_{111}^2 X_1^3 + h_{112}^2 X_1^2 X_2 + h_{122}^2 X_1 X_2^2 + h_{222}^2 X_2^3 = 0. \tag{1b}$$

In the above system, $(X_1(t), X_2(t))$ are the displacements of the two DOFs at time $t$, $\dot{} = \mathrm{d}\cdot/\mathrm{d}t$ is the time derivative, and $(g_{ij}^k, h_{ijl}^k)$, $i,j,l,k = 1,2$ are the coefficients of the quadratic and cubic terms. This kind of system is encountered in many fields of physics and engineering [2, 4] and especially when reducing the dynamics of curved thin mechanical structures such as shells and arches, the curvature being responsible of the appearance of the quadratic terms [27–29]. Here, all possible quadratic and cubic terms are considered, without restriction on their values. In particular, the case for which Eq. (1) derive from a potential leads to known relationships between some of the coefficients, such that finally, only nine free coefficients remains in this case, which is recalled in "Appendix A", see also e.g. [2, 30]. Note however that this specific case is not considered here for the sake of generality, and also because in some of the targeted applications, the nonlinear terms are artificially created; see e.g. the case of electronic circuits for vibration control applications [17, 31].

### 2.1 Real normal form up to the third order with a second-order resonance

The aim of this section is to derive the normal form of Eq. (1) up to cubic terms, in the specific case where a 1:2 internal resonance exists between the two eigenfrequencies of the problem, such that the relationship $\omega_2 \approx 2\omega_1$ holds. The theory of normal form has been used for a long time for vibratory problems, in order to simplify as much as possible the dynamical system under study by cancelling all the non-resonant monomials thanks to a nonlinear change of coordinates, see e.g. [19, 21, 32, 33]. It has also been used in the context of model order reduction to underline the link with nonlinear normal modes (NNMs), defined as invariant manifolds in phase space [11, 23, 27]. Importantly, different *styles* of normal form exist due to the non-uniqueness of the solutions of the homological equations, and the freedom of choosing one solution or another leads to the idea of *free functions*, as explained for example in [22, 34].

Focusing on the case of vibratory problems where the eigenspectrum is composed of pairs of complex conjugate eigenvalues, three main different styles of normal forms can be distinguished. The first one is the complex normal form, as first introduced in [19], which is closer to the formulas used in the dynamical system community, see e.g. [21, 33, 35]. The second one is the real normal form introduced in [20, 34, 36], which allows one to retrieve more easily oscillator equations. The third one is a full real normal form, first introduced in [11, 23], where the oscillator form of the equations is strongly enforced throughout the calculation, imposing the variables to stay homogeneous to a displacement and a velocity. Further comments on these different normal forms can also be found in [37], in the context of the parameterisation method for invariant manifolds. In this article, this third normal form will be used to simplify Eq. (1).

A generic calculation, up to cubic order, and including detailed analytical formulas for all the coefficients of the nonlinear mappings and normal form, has already been provided in [11, 38] for conservative problems, and in [12, 23] for assemblies of damped nonlinear oscillators. However, this calculation is led to the case where no internal resonance exists between the eigenfrequencies of the problem. In the case where a second-order internal resonance exist, like the 1:2 resonance considered here, the calculation needs to be adapted. In particular, the cubic terms need to be recomputed to take into account the resonant monomials of second order that are due to the 1:2 resonance. In turn, these resonant terms will modify some coefficients used for the change of coordinates, and some of the cubic terms of the normal

form. The aim of this section is thus to enlarge the general results provided in [11] to the case of a 1:2 resonance.

For the sake of conciseness, only the result of this calculation is given here in the main text. The interested reader can find the full demonstration and the complete calculation in "Appendix B". The real normal form of Eq. (1), up to cubic order, with a 1:2 internal resonance between the two eigenfrequencies ($\omega_2 \approx 2\omega_1$), reads:

$$\begin{aligned}&\ddot{R}_1 + \omega_1^2 R_1 + g_{12}^1 R_1 R_2 + (h_{111}^1 + A_{111}^1) R_1^3 + (h_{122}^1 + A_{122}^1) R_1 R_2^2 \\ &\quad + B_{111}^1 R_1 \dot{R}_1^2 + B_{122}^1 R_1 \dot{R}_2^2 + B_{212}^1 R_2 \dot{R}_1 \dot{R}_2 = 0,\end{aligned} \tag{2a}$$

$$\begin{aligned}&\ddot{R}_2 + \omega_2^2 R_2 + g_{11}^2 R_1^2 + (h_{112}^2 + A_{112}^2 - D_{112}^2) R_1^2 R_2 + (h_{222}^2 + A_{222}^2) R_2^3 \\ &\quad + (B_{112}^2 - E_{112}^2) R_1 \dot{R}_1 \dot{R}_2 + B_{211}^2 R_2 \dot{R}_1^2 + B_{222}^2 R_2 \dot{R}_2^2 = 0.\end{aligned} \tag{2b}$$

In these equations, $(R_1, R_2)$ are the *normal* coordinates, homogeneous to a displacement. These new coordinates are nonlinearly related to the original ones thanks to an identity-tangent nonlinear mapping. For completeness, the nonlinear change of coordinate needs to consider both the displacements (original displacement with $X_p$ coordinate and normal displacement with $R_p$, $p$=1,2) and the velocities, here written as $Y_p = \dot{X}_p$ for the original coordinates, and $S_p = \dot{R}_p$ for the normal ones. The nonlinear mappings read, for $p$=1,2:

$$\begin{aligned}X_p = R_p &+ \sum_{i=1}^{2}\sum_{j\geq i}^{2} a_{ij}^p R_i R_j + \sum_{i=1}^{2}\sum_{j\geq i}^{2} b_{ij}^p S_i S_j + \sum_{i=1}^{2}\sum_{j\geq i}^{2}\sum_{k\geq j}^{2} r_{ijk}^p R_i R_j R_k \\ &+ \sum_{i=1}^{2}\sum_{j=1}^{2}\sum_{k\geq j}^{2} u_{ijk}^p R_i S_j S_k,\end{aligned} \tag{3a}$$

$$\begin{aligned}Y_p = S_p &+ \sum_{i=1}^{2}\sum_{j=1}^{2} \gamma_{ij}^p R_i S_j + \sum_{i=1}^{2}\sum_{j\geq i}^{2}\sum_{k\geq j}^{2} \mu_{ijk}^p S_i S_j S_k \\ &+ \sum_{i=1}^{2}\sum_{j=1}^{2}\sum_{k\geq j}^{2} \nu_{ijk}^p S_i R_j R_k.\end{aligned} \tag{3b}$$

The expressions of all the introduced coefficients in Eq. (3) are given in "Appendix B", following the general formulas given in [11]. In Eq. (2), only the resonant monomials are present. Due to the 1:2 internal resonance, only two quadratic monomials are present, instead of the six in the original Eq. (1). Due to the asymptotic nature of the normal form calculation, which eliminates the non-resonant terms order by order, the coefficients of the cubic terms are modified by the appearance of $A_{ijk}^p$, $B_{ijk}^p$, $D_{ijk}^p$ and $E_{ijk}^p$. The first two coefficients $A_{ijk}^p$ and $B_{ijk}^p$ have already been considered in [11], and their expressions read:

$$A_{ijk}^p = \sum_{l\geq i}^{N} g_{il}^p a_{jk}^l + \sum_{l\leq i}^{N} g_{li}^p a_{jk}^l, \tag{4a}$$

$$B_{ijk}^p = \sum_{l\geq i}^{N} g_{il}^p b_{jk}^l + \sum_{l\leq i}^{N} g_{li}^p b_{jk}^l. \tag{4b}$$

One can note in particular that these two coefficients appear due to the elimination of the non-resonant quadratic terms, hence they involve only quadratic original $g_{ij}^p$ coefficients, with the coefficients of the quadratic part of the nonlinear mappings: $a_{jk}^p$ and $b_{jk}^p$. The last two terms, $D_{ijk}^p$ and $E_{ijk}^p$, are new as compared to the general results presented in [11], and their presence is only due to the existence of the 1:2 internal resonance and the two resonant quadratic monomials in the normal form. Their expressions write:

$$D_{112}^2 = \gamma_{22}^2 g_{11}^2 - 2b_{22}^2 g_{11}^2 \omega_2^2, \tag{5a}$$

$$E_{112}^2 = 4b_{22}^2 g_{11}^2. \tag{5b}$$

The remainder of the paper consists in analyzing the solutions of the normal form of the system with 1:2 internal resonance and up to cubic terms, Eq. (2). A particular emphasis will be set to understand the effect of the *non-resonant* quadratic monomials on the dynamical characteristics of the system. Note that these non-resonant monomials have been cancelled in Eq. (2). However, the associated coefficients $g_{ij}^p$ intervene in the cubic terms, and will thus have an important effect on backbone curves and frequency response functions. The analysis will be done using a multiple scales solution up to the second-order to take the cubic terms into account.

### 2.2 Multiple scales solution: modulation equations

In this section, an approximate analytical solution of the normal form system (2), using the multiple scales method (MSM), is proposed. Analytical solutions of 1:2 internally resonant problems have been proposed in many instances, for example, with the MSM for

first and second-order developments [1, 39]. They are, however, generally restricted to the case with forcing and damping, and cubic terms are generally not taken into account. Besides, the study of the backbones for free vibration problems has been only recently considered, see e.g. [10, 13], but still without considering the cubic terms. The main aim of the development proposed here is to extend these latter results by including the effect of cubic terms, in the presence of 2:1 internal resonance. For other types of internal resonance, such as 1:1 internal resonance, one can refer to [40], where detailed second-order MSM derivations are established to obtain the free solution of Eq. (1), considering all the quadratic and cubic terms.

Eq. (2) are first rewritten by introducing a small bookkeeping parameter $\varepsilon$ in order to scale the different nonlinear terms as:

$$\ddot{R}_1 + \omega_1^2 R_1 = -\varepsilon\beta_1 R_1 R_2 - \varepsilon^2\left[\alpha_1 R_1^3 + \alpha_2 R_1 R_2^2 + \alpha_3 R_1 \dot{R}_1^2 + \alpha_4 R_1 \dot{R}_2^2 + \alpha_5 R_2 \dot{R}_1 \dot{R}_2\right], \tag{6a}$$

$$\ddot{R}_2 + \omega_2^2 R_2 = -\varepsilon\beta_2 R_1^2 - \varepsilon^2\left[\alpha_6 R_1^2 R_2 + \alpha_7 R_2^3 + \alpha_8 R_1 \dot{R}_1 \dot{R}_2 + \alpha_9 R_2 \dot{R}_1^2 + \alpha_{10} R_2 \dot{R}_2^2\right], \tag{6b}$$

where the coefficients $\alpha_k$, $k = 1, \dots 10$ have been simply introduced from Eq. (2), see Eq. (50) in "Appendix C" for their detailed expressions.

The second-order expansion using MSM requires the definition of three time scales $T_0 = t$, $T_1 = \varepsilon t$, and $T_2 = \varepsilon^2 t$. Following the method (see "Appendix C" for details), the free solution is approximated as:

$$R_1(t) = a_1(T_1, T_2)\cos(\omega_1 T_0 + \theta_1(T_1, T_2)) + O(\varepsilon), \tag{7a}$$

$$R_2(t) = a_2(T_1, T_2)\cos(\omega_2 T_0 + \theta_2(T_1, T_2)) + O(\varepsilon), \tag{7b}$$

where $a_1$, $a_2$, $\theta_1$ and $\theta_2$ are real functions of the slow time scales only $(T_1, T_2)$. The nearness of the internal resonance condition leads to define the internal detuning parameter $\sigma$ as:

$$\varepsilon\sigma = 2\omega_1 - \omega_2. \tag{8}$$

The complete derivation is reported in "Appendix C" for the sake of brevity. Solvability conditions are obtained by eliminating resonant terms both at orders $\varepsilon$ and $\varepsilon^2$, leading respectively to two sets of equations of the form $D_1 A = \dots$ and $D_2 A = \dots$ for each of the slow time scales (where $D_1$ and $D_2$ refers to a partial derivative with respect to $T_1$ and $T_2$). These two sets of equations can be recombined using the so-called reconstitution method [39, 41], yielding:

$$\dot{A} = \frac{\mathrm{d}A}{\mathrm{d}t} = \varepsilon D_1 A + \varepsilon^2 D_2 A + O(\varepsilon^3), \tag{9}$$

for any complex amplitude $A(T_1, T_2)$. After some algebra, detailed in "Appendix C", one obtains the following slow time scale modulation equations:

$$\dot{a}_1 = \frac{\varepsilon\beta_1 a_1 a_2}{4\omega_1}\left[1 + \frac{\varepsilon\sigma}{2\omega_1}\right]\sin\gamma_p, \tag{10a}$$

$$\dot{a}_2 = -\frac{\varepsilon\beta_2 a_1^2}{4\omega_2}\left[1 - \frac{\varepsilon\sigma}{2\omega_2}\right]\sin\gamma_p, \tag{10b}$$

$$\dot{\theta}_1 = \frac{\varepsilon\beta_1 a_2}{4\omega_1}\left[1 + \frac{\varepsilon\sigma}{2\omega_1}\right]\cos\gamma_p - \varepsilon^2\frac{\Lambda_1 a_2^2 + \Lambda_2 a_1^2}{8\omega_1}, \tag{10c}$$

$$\dot{\theta}_2 = \frac{\varepsilon\beta_2 a_1^2}{4\omega_2 a_2}\left[1 - \frac{\varepsilon\sigma}{2\omega_2}\right]\cos\gamma_p - \varepsilon^2\frac{\Lambda_3 a_1^2 + \Lambda_4 a_2^2}{8\omega_2}, \tag{10d}$$

where

$$\gamma_p = 2\theta_1 - \theta_2 + \sigma T_1. \tag{11}$$

Note that these recombined equations now explicitly depend on both quadratic terms, via the $(\beta_1, \beta_2)$ coefficients; and cubic terms, via the newly introduced coefficients $\Lambda_k$, $k = 1, \dots 4$, which read:

$$\Lambda_1 = -\beta_1^2\left[\frac{1}{4\omega_1^2} + \frac{1}{\omega_2(2\omega_1 + \omega_2)}\right] - 2\alpha_4\omega_2^2 - 2\alpha_2, \tag{12a}$$

$$\Lambda_2 = \beta_1\beta_2\left[\frac{1}{4\omega_1\omega_2} + \frac{2}{\omega_2^2}\right] - \alpha_3\omega_1^2 - 3\alpha_1, \tag{12b}$$

$$\Lambda_3 = \beta_1\beta_2\left[\frac{1}{2\omega_1\omega_2} - \frac{2}{\omega_2(2\omega_1 + \omega_2)}\right] - 2\alpha_6 - 2\alpha_9\omega_1^2, \tag{12c}$$

$$\Lambda_4 = -3\alpha_7 - \alpha_{10}\omega_2^2. \tag{12d}$$

On can remark as a particular feature that the coefficients $\alpha_5$ and $\alpha_8$ do not appear in the above $\Lambda_i$ expressions, even though they are associated to resonant

cubic monomials in the real normal form. The MSM expansion shows that their effect is seen from the next order of development. As a matter of fact, real normal form differs from complex normal form, is less symmetric, and produces more resonant monomials. Also, the MSM expansion, using complex notations, implicitly relies on the complex normal form, and expresses the resonant monomials through the solvability condition. Hence it can be concluded that the monomials associated with $\alpha_5$ and $\alpha_8$ are resonant for the real normal form, but not for the complex normal form, explaining the fact that they disappear when one writes down the modulation equation with the MSM.

Since $\gamma_p$ explicitly depends on the slow time scale $T_1$, the system defined by Eqs. (10a–10d) is not autonomous. Then, it is convenient to combine the phase Eqs. (10c,10d) with (11) to obtain:

$$\dot{\gamma}_p = \varepsilon\sigma + \left(\frac{\varepsilon\beta_1 a_2}{2\omega_1}\left[1+\frac{\varepsilon\sigma}{2\omega_2}\right] - \frac{\varepsilon\beta_2 a_1^2}{4a_2\omega_2}\left[1-\frac{\varepsilon\sigma}{2\omega_2}\right]\right)\cos\gamma_p + \varepsilon^2\left(\frac{\Lambda_3 a_1^2+\Lambda_4 a_2^2}{8\omega_2} - \frac{\Lambda_1 a_2^2+\Lambda_2 a_1^2}{4\omega_1}\right), \tag{13}$$

in which $\mathrm{d}T_1/\mathrm{d}t = \varepsilon$ has been used. Consequently, one obtains two equivalent *autonomous systems*, being, respectively Eqs. (10a, 10b, 10c)–(13) in term of variables $(a_1, a_2, \theta_1, \gamma_p)$ and Eqs. (10a, 10b, 10d)–(13) in term of variables $(a_1, a_2, \theta_2, \gamma_p)$. This generic four-dimensional dynamical system will be reduced to a three-dimensional one in the next section, in the particular case of stationary solutions. One must also remark that Eqs. (10c, 10d) (and consequently Eq. (13)) are valid only if $a_1, a_2 \neq 0$ since they result from Eqs. (62c, 62d) divided respectively by $a_1$ and $a_2$.

Now that the modulation equations have been derived, the focus will be on analyzing their solutions. Before proceeding in the next section, it is worth underlining that the quadratic terms in Eq. (62) are the same as those reported in [10], obtained with a first-order MSM solution, hence highlighting how the results presented here will extend earlier derivations. Another important point, discussed in "Appendix C and E", is that these modulation equations are slightly different from those obtained in previous studies, see e.g. Eqs. (175–178) of [39], in which a similar problem is considered through a second-order MSM solution. The discrepancies are the consequence of the different assumptions used in the MSM process. In particular, alternative derivations, as those presented in [39], have been deeply analyzed and compared to the ones presented here, and "Appendix E" is completely devoted to these calculations, which clearly show that the retained assumptions lead to better results as compared to reference numerical solutions, justifying our final choice.

### 2.3 Branches of stationary solutions

Integrating the modulation Eq. (10) can lead to various free vibration solutions, depending on the four initial conditions $R_1(0)$, $R_2(0)$, $\dot{R}_1(0)$, $\dot{R}_2(0)$. Restricting ourselves to solutions that are stationary in amplitude, *i.e.* such that $\mathrm{d}a_1/\mathrm{d}t = \mathrm{d}a_2/\mathrm{d}t = 0$, imposes a stringent condition on the phase $\gamma_p$, since non trivial solutions are obtained when $\sin\gamma_p = 0$, which implies that $\gamma_p$ *is also stationary*, with value $\gamma_p = k\pi$ with $k \in \mathbb{Z}$ and $\cos\gamma_p = p$ with $p = \pm 1$.

Then, because $a_1$, $a_2$ and $\gamma_p$ are constants, one obtains three conditions. The second member of Eq. (10c, 10d) are constants, which leads to the first two:

$$\dot{\theta}_1 = \tilde{\omega}_1 = \Gamma_1 p\, a_2 + \Gamma_2 a_1^2 + \Gamma_3 a_2^2 \quad \Rightarrow \quad \theta_1(t) = \tilde{\omega}_1 t + \phi_1; \tag{14a}$$

$$\dot{\theta}_2 = \tilde{\omega}_2 = \Gamma_4 p\,\frac{a_1^2}{a_2} + \Gamma_5 a_1^2 + \Gamma_6 a_2^2 \quad \Rightarrow \quad \theta_2(t) = \tilde{\omega}_2 t + \phi_2, \tag{14b}$$

where $\phi_1$ and $\phi_2$ are integration constants and the coefficients $\Gamma_k$, $k = 1, \ldots 6$ are functions of the system's parameters. Their expression naturally appear in the modulation equations in the process of the MSM, see "Appendix C" for details, and their explicit expressions read:

$$\Gamma_1 = \frac{\varepsilon\beta_1}{4\omega_1}\left[1+\frac{\varepsilon\sigma}{2\omega_1}\right], \quad \Gamma_4 = \frac{\varepsilon\beta_2}{4\omega_2}\left[1-\frac{\varepsilon\sigma}{2\omega_2}\right], \tag{15a}$$

$$\Gamma_2 = -\frac{\varepsilon^2\Lambda_2}{8\omega_1}, \quad \Gamma_3 = -\frac{\varepsilon^2\Lambda_1}{8\omega_1}, \quad \Gamma_5 = -\frac{\varepsilon^2\Lambda_3}{8\omega_2}, \quad \Gamma_6 = -\frac{\varepsilon^2\Lambda_4}{8\omega_2}. \tag{15b}$$

Finally, the third condition is the following relationship between $a_1$ and $a_2$, obtained with Eqs. (11), (14a, 14b):

$$\dot{\gamma}_p = 2\tilde{\omega}_1 - \tilde{\omega}_2 + \varepsilon\sigma = 0 \quad \Rightarrow \quad a_1^2 = \frac{(2\omega_1 - \omega_2)a_2 + 2\Gamma_1 p\, a_2^2 + (2\Gamma_3 - \Gamma_6)a_2^3}{\Gamma_4 p + (\Gamma_5 - 2\Gamma_2)a_2}. \tag{16}$$

Then, eliminating $(\theta_1, \theta_2)$ in Eqs (7a, 7b) with Eqs. (14a–14b), one obtains:

$$R_1(t) = a_1 \cos\left(\omega_{\text{nl1}} t + \phi_1\right) + O(\varepsilon), \tag{17a}$$

$$R_2(t) = a_2 \cos\left(\omega_{\text{nl2}} t + \phi_2\right) + O(\varepsilon), \tag{17b}$$

where the nonlinear frequencies are functions of the amplitudes as follows:

$$\omega_{\text{nl1}} = \omega_1 + \Gamma_1 p\, a_2 + \Gamma_2 a_1^2 + \Gamma_3 a_2^2, \tag{18a}$$

$$\omega_{\text{nl2}} = \omega_2 + \Gamma_4 p \frac{a_1^2}{a_2} + \Gamma_5 a_1^2 + \Gamma_6 a_2^2. \tag{18b}$$

One can notice that the obtained solutions are families of periodic orbits, with frequencies $\omega_{\text{nl1}}$ and $\omega_{\text{nl2}}$ depending on the amplitudes $a_1$ and $a_2$. The frequency dependence upon amplitudes given in Eq. (18) defines the two backbone curves of the coupled solutions of the system. In phase space, the corresponding families of periodic orbits lie on invariant manifolds known as a Lyapunov Subcenter Manifold (LSM) in this conservative case [27]. This LSM is univocally defined as a nonlinear mode (NNM) in vibration theory [11, 12, 27, 42, 43].

Based on the above developments, several solutions can be found:

- The trivial solution $a_1 = a_2 = 0$;
- An uncoupled solution with $(a_1 \neq 0, a_2 = 0)$, denoted as the U1-mode. Eq. (62d) shows that $a_2 = 0 \Rightarrow a_1 = 0$ so that this U1-mode is not admissible[1]. Going back to the initial system (6), this result is natural since a quadratic invariance breaking term $\beta_2 R_1^2$ is present in the second equation. Consequently, the U1-mode does not exist as a possible solution of the system.
- An uncoupled solution with $(a_1 = 0, a_2 \neq 0)$, denoted as the U2-mode. This solution is possible and corresponds to the single mode vibration of the second mode. Since it is dictated by a nonlinear oscillator, on can easily derives the uncoupled backbone curve of the U2-mode from Eq. (18b) as

$$\omega_{\text{nl2}} = \omega_2 \left(1 + \frac{\Gamma_6}{\omega_2} a_2^2\right). \tag{19}$$

The backbone curve of the U2-mode, obtained by imposing $R_1 = 0$ in the second equation of the initial system (6b), has thus a hardening/softening behaviour dictated by the sign of $\Gamma_6$.

- a coupled solution with $(a_1 \neq 0, a_2 \neq 0)$, denoted as C− mode. In this case, the fact that $\gamma_p$ is a constant, see Eq. (16), shows that the *oscillations of the two DOFs are locked*, in *frequency and phase*:

$$\omega_{\text{nl1}} = \omega_{\text{nl2}}/2, \quad \phi_1 = (\phi_2 + k\pi)/2, \tag{20}$$

as well as in *amplitude* since $a_1$ is a function of $a_2$ thanks to Eq. (16). At this stage, one must remember that two values for $\cos\gamma_p = p = \pm 1$ are admissible, leading to *two distinct coupled modes*: the C+ mode, with $p = 1$, $k$ even and the C− mode, with $p = -1$, $k$ odd. An interesting consequence of the locking is the shape of those C+ and C− modes in the configuration space $(R_1, R_2)$. Using Eq. (20) in Eqs. (17a, 17b), one obtains:

$$R_1(t) = a_1 \cos\left(\frac{\omega_{\text{nl2}}}{2} t + \frac{\phi_2 + k\pi}{2}\right) + O(\varepsilon), \tag{21a}$$

$$R_2(t) = a_2 \cos\left(\omega_{\text{nl2}} t + \phi_2\right) + O(\varepsilon), \tag{21b}$$

from which one easily shows that:

$$\text{C+ mode:} \quad \frac{R_2}{a_2} = 2\frac{R_1^2}{a_1^2} - 1; \qquad \text{C − mode:} \quad \frac{R_2}{a_2} = -2\frac{R_1^2}{a_1^2} + 1. \tag{22}$$

The two above equations show that the two modes have the shape of parabolas in the space $(R_1, R_2)$, as shown in Fig. 1, a result that has already been underlined in [10], but using a first-order MSM on a quadratic system. Analogous results on the topology of coupled modes were also obtained in the case of 1:1 internal resonance, where the modes were denoted, depending on their shape

[1] One cannot use directly Eq. (14b), since it is valid only if $a_1, a_2 \neq 0$

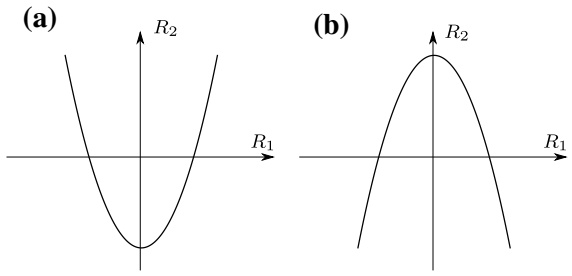


**Fig. 1** Parabolic Modes of the coupled solutions in the configuration plane $(R_1(t), R_2(t))$. **a** the C+ mode and **b** the C− mode

in the configuration space, as "normal mode" and "elliptic mode" [44, 45].

The main difference in the results reported here, as compared, for example, to the recent ones on the backbone curves derived in [10], lies in the fact that cubic terms are taken into account thanks to the normal form approach and the second-order MSM. The main consequence is that the backbone curve of the U2-mode has a curvature and is not a straight line anymore, because of the cubic term. In the same context, the coupled backbones of the C+ and C− modes will show a curvature, a feature that was not present in [10].

### 2.4 Existence conditions and branching of the coupled solution

This section is devoted to the derivation of results on the existing conditions of the C+ and C− modes and their branching to the U2-mode. Only the mathematical derivations are given, illustrative examples being postponed to Sect. 3.1 where a special emphasis on the topology of the bifurcated solutions will be given.

Starting with the uncoupled solution (U2-mode), one easily observes that there are no restriction that might give rise to a condition of existence. The discussion can thus focus on the case of the coupled C+ and C− modes. A simple condition is derived by imposing that the expression of $a_1^2$ in Eq. (16) must be positive. For the ease of the discussion, let us first consider the simplified case of the first-order MSM solution, already analyzed in [10]. This case is obtained by dropping all $\varepsilon^2$ terms in Eq. (15), leading to $\Gamma_1 = \varepsilon\beta_1/(4\omega_1)$, $\Gamma_4 = \varepsilon\beta_2/(4\omega_2)$ and $\Gamma_2 = \Gamma_3 = \Gamma_5 = \Gamma_6 = 0$. The positive sign of $a_1^2$ from Eq. (16) depends on the signs of $\beta_1$ and $\beta_2$, leading to the two following conditions that enforces $a_1^2 \geq 0$:

$$\begin{aligned} &\text{sign}\beta_1 = \text{sign}\beta_2 \Rightarrow a_2 \geq -p\zeta_0; \\ &\text{sign}\beta_1 \neq \text{sign}\beta_2 \Rightarrow a_2 \leq -p\zeta_0, \end{aligned} \tag{23}$$

with

$$\zeta_0 = \frac{2\omega_1 - \omega_2}{2\Gamma_1} = \frac{2\omega_1(2\omega_1 - \omega_2)}{\varepsilon\beta_1} = \frac{2\omega_1\sigma}{\beta_1}. \tag{24}$$

Hence in this simplified case, $-p\zeta_0$ appears as the unique root where $a_1^2$ vanishes in Eq. (16). Since we can consider $a_2 > 0$ without loss of generality, the coupled backbones exist only if $\beta_1$ and $\beta_2$ share the same sign, and one of the coupled backbones is defined for $a_2 \geq 0$ whereas the other exists for $a_2 \geq |\zeta_0|$ (reminding that $p = \pm 1$). In this latter case, $a_2 = |\zeta_0|$ leads to $a_1 = 0$ and to $\omega_{\text{nl}2} = \omega_2$, which means that one of the coupled backbones emerges from the uncoupled U2-mode backbone curve (which is in this simplified case the vertical line $\omega_{\text{nl}2} = \omega_2$) at a non zero amplitude $a_2 = |\zeta_0|$. In the special case of $\sigma = 0$, both backbones emerge at a vanishing amplitude, and from the x-axis (referring to the frequency) at the same point as $\omega_2 = 2\omega_1$.

Let us now analyze the more difficult present case of the solutions at second order. In this case, the situation is less straightforward since it depends on all six nonzero $\Gamma_k$ coefficients. Requiring that $a_1^2$ is positive in Eq. (16) leads to the following condition:

$$L(a_2) \equiv a_2\Big[(2\omega_1 - \omega_2) + 2\Gamma_1 p\, a_2 + (2\Gamma_3 - \Gamma_6)a_2^2\Big]\Big[\Gamma_4 p + (\Gamma_5 - 2\Gamma_2)a_2\Big] \geq 0, \tag{25}$$

where $L(a_2)$ is the product of the numerator and denominator of the right-hand side of Eq. (16). The roots of the polynomial $L(a_2)$ are:

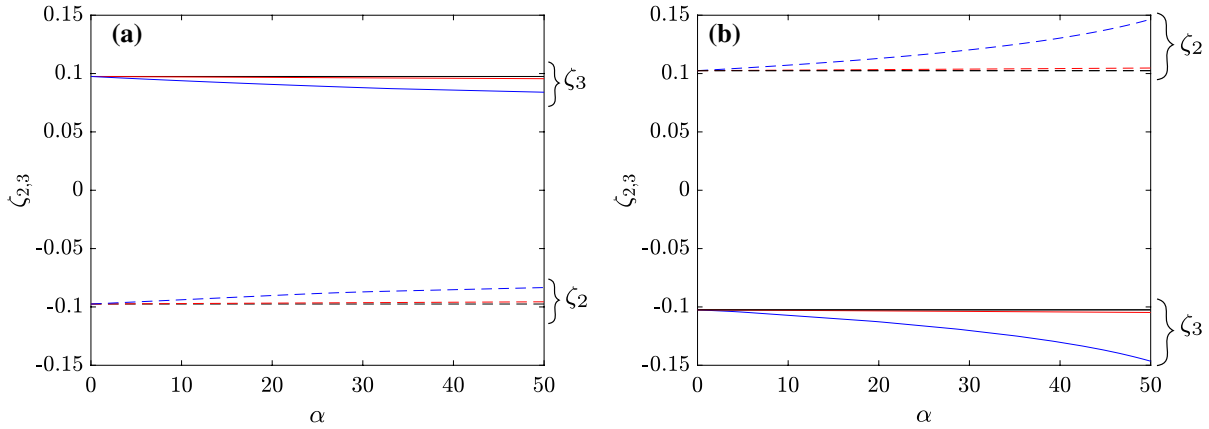


**Fig. 2** Behaviour of the roots $\zeta_{2,3}$ as function of the cubic $\alpha$ coefficient taken with equal values for simplicity ($\alpha = \alpha_k\ \forall k$) and with $\beta_1 = \beta_2 = 1$. Solid lines refers to the C+ mode with $p = 1$, while dashed lines refers to the C− mode with $p = -1$. The red and blue lines denote respectively the case with $\varepsilon = 0.001$ and $\varepsilon = 0.01$. The black line denotes $-p\zeta_0$. (**a**) case of a negative detuning with $\omega_2 = 2$ and $\omega_1 = 0.975$, (**b**) case of a positive detuning with $\omega_2 = 2$ and $\omega_1 = 1.025$. (Color figure online)

$$\zeta_1 = \frac{\Gamma_4 p}{2\Gamma_2 - \Gamma_5}, \quad \zeta_{2,3} = \frac{1}{\Gamma_6 - 2\Gamma_3}\left[\Gamma_1 p \pm \sqrt{\Gamma_1^2 + (2\omega_1 - \omega_2)(\Gamma_6 - 2\Gamma_3)}\right], \tag{26}$$

in addition to the vanishing solution. The two roots $\zeta_{2,3}$ are important since they come from the numerator of $a_1^2$, such that they nullify $a_1$ ($a_2 = \zeta_{2,3} \Rightarrow a_1 = 0$). In comparison to the above considered first-order MSM results, the three roots $\zeta_{1,2,3}$ are obtained instead of the single root $-p\zeta_0$. Note that, as long as $\varepsilon$ is small, the second-order MSM solution is a correction to the first-order, and thus should not change the situation drastically. In particular, in the spirit of perturbative reasoning based on the leading orders, one can easily assume that $\Gamma_2$, $\Gamma_3$, $\Gamma_5$, and $\Gamma_6$ are small. Consequently, since the denominators $2\Gamma_2 - \Gamma_5$ and $\Gamma_6 - 2\Gamma_3$ are small, one of the two roots, either $\zeta_2$ or $\zeta_3$, should be close to $-p\zeta_0$, whereas the two others, either $\zeta_2$ or $\zeta_3$ in addition to $\zeta_1$, are far from $-p\zeta_0$ in absolute value. As a consequence, we can conjecture by perturbative reasoning that the starting point of the coupled backbone curves in the plane $(\omega_{\text{nl2}}, a_2)$ admits an amplitude of $\zeta_2$ (or $\zeta_3$) and represents a branching point from the uncoupled backbone curves.

To illustrate the above reasoning, we assume an equal value for all cubic coefficients $\alpha_i = \alpha$, $\forall i = 1, \ldots 10$ to control the amount of cubic terms with a single parameter. Then, Fig. 2 shows the evolution of the roots $\zeta_{2,3}$ from Eq. (26), and $-p\zeta_0$, from Eq. (24) as a function of $\alpha$ for two different values of $\varepsilon$ and two different values of the detuning. It clearly shows that the new roots $\zeta_{2,3}$ of the second-order analysis emerge from the root $-p\zeta_0$ of the first-order analysis, hence validating the above perturbative reasoning. This will be further illustrated in Figs. 3 and 4 in the next section, showing undoubtedly that the coupled backbone that starts at a non-zero-amplitude branches from the uncoupled U2 mode. With a calculation, this can be verified by substituting $a_2$ from the numerator of Eq. (16), which defines $\zeta_{2,3}$, in (18a), to obtain Eq. (19).

Note that in the special case of $\sigma = 0$ ($\omega_2 = 2\omega_1$), $\zeta_1$ is given by Eq. (26) and the two roots reads:

$$\zeta_{2,3} = 0 \quad \text{or} \quad \frac{2p\Gamma_1}{\Gamma_6 - 2\Gamma_3}, \tag{27}$$

With the same reasoning, since $\Gamma_6 - 2\Gamma_3$ is small with respect to $\Gamma_1$, $\zeta_0 = 0$ is replaced here by $\zeta_{2,3} = 0$, showing that the branching point between the U2-mode and the coupled-mode backbones appears at $a_2 = 0$.

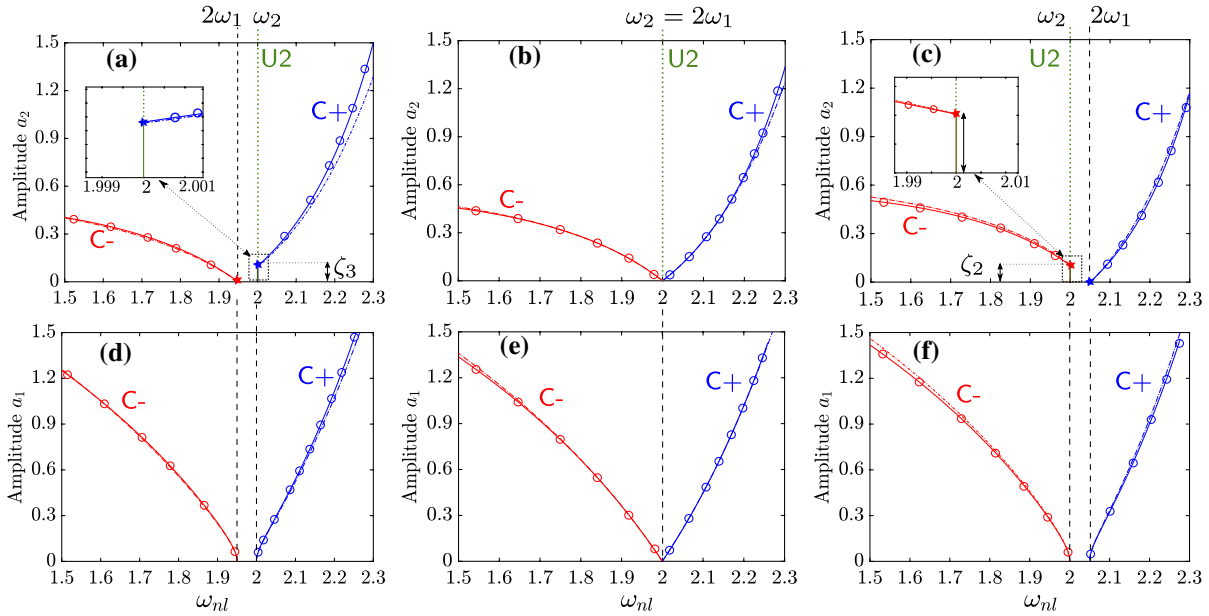


**Fig. 3** Backbone curves of the system in the specific case where only the quadratic resonant terms are considered such that $g^1_{12} = g^2_{11} = 1$, while the other nonlinear coefficients are zero. Three different detunings are analyzed: $\sigma = -0.05$ (first column), $\sigma = 0$ (second column), and $\sigma = 0.05$ (third column). Comparison between the second-order MSM result (dash-dotted) and the reference numerical solution directly obtained from the normal form (2a–d) (solid line with circle markers). Coupled solutions, C+ mode and C− mode, are plotted in blue and red, respectively. The uncoupled solution (U2 mode) is plotted in green with solid and dotted lines denote the stable and unstable solutions, respectively. (Color figure online)

All these results complement and extend those given in [10]. In particular, the fact that the branch point of the coupled backbones lies on the uncoupled one was not demonstrated in [10]. Moreover, we have shown here that the result extends when considering the cubic terms. The main difference is that under such assumption, the backbone curve of the U2-mode is now curved (thanks to the cubic term). However, the branching point of the C+/C− solution remains on the same uncoupled backbone.

### 2.5 Stability of the coupled C+ and C− solutions

The stability of the solutions requires computing the eigenvalues of the Jacobian of the modulation equations. For the ease of the solution, it appears more convenient to compute this Jacobian for the underlying three-dimensional autonomous system obtained from the two amplitude Eqs. (10a, 10b), complemented with the angular Eq. (13) (see "Appendix C" for the calculation details). Since there is no damping in the system, the stability is assessed if the eigenvalues are either zero or purely imaginary, leading to a neutrally stable fixed point [4].

In the case of the coupled C+ and C− solutions, the Jacobian is written in "Appendix D" and leads to the eigenvalues:

$$\lambda_1 = 0, \quad \lambda_{2,3} = \pm a_1 \sqrt{\nu a_2 - \Gamma_4^2 \frac{a_1^2}{a_2^2} - 4\Gamma_1\Gamma_4}, \qquad (28)$$

with

$$\nu = 2\Gamma_4\, p\,(\Gamma_6 - 2\Gamma_3) + 2\Gamma_1\, p\,(2\Gamma_2 - \Gamma_5). \qquad (29)$$

In the most general case of arbitrary coefficients $\Gamma_k$, assessing the sign of the radicand is difficult. More simple reasoning can be conducted with a perturbative approach, as in the previous section. Indeed, if $\varepsilon$ is small, then $\Gamma_{2,3,5,6}$ are also small with respect to $\Gamma_{1,4}$. Consequently at first-order (thus coinciding with the solution analyzed in [10]), the eigenvalues simplifies to $\lambda_{2,3} \simeq \pm a_1 \sqrt{-\Gamma_4^2 a_1^2/a_2^2 - 4\Gamma_1\Gamma_4}$. If $\beta_1$ and $\beta_2$ share the same sign, it is also the case for $\Gamma_1$ and $\Gamma_4$ and one

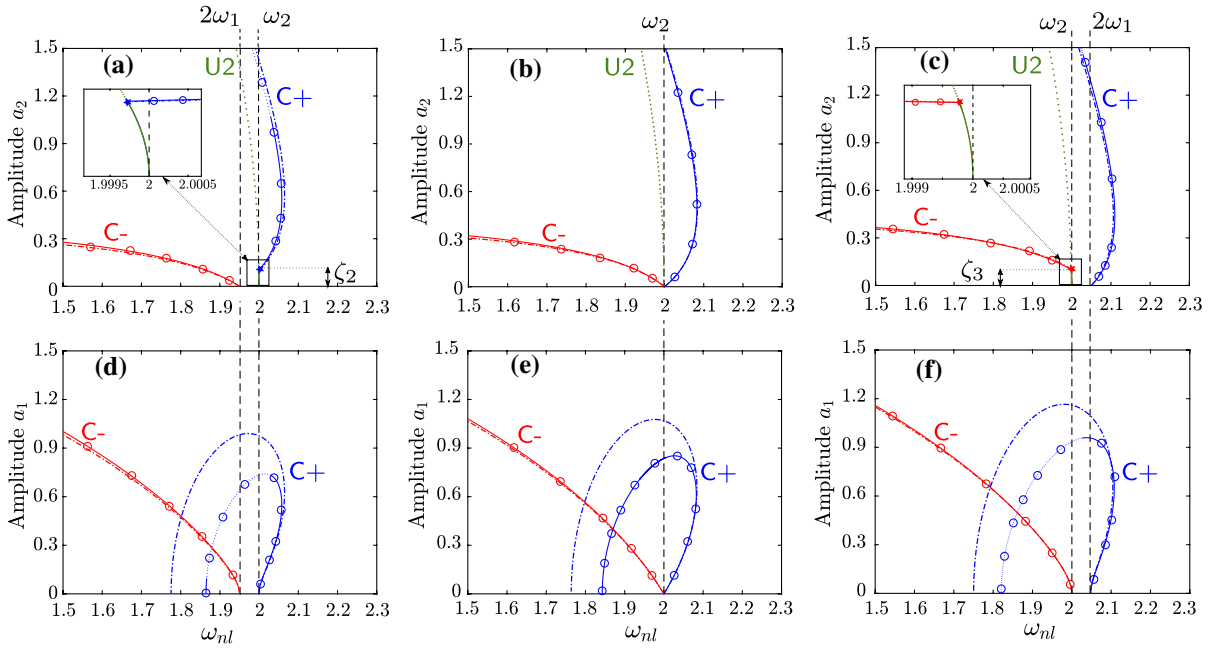


**Fig. 4** Backbone curves of the system with quadratic and cubic terms considered: $g^1_{12} = g^2_{11} = 1$, $g^1_{11} = g^1_{22} = g^2_{12} = g^2_{22} = 0.5$, and $h^p_{ijk} = 0.1$ for $i$, $j$, $k$, and $p = 1, 2$. Three different detunings are considered: $\sigma = -0.05$ (first column), $\sigma = 0$ (second column), and $\sigma = 0.05$ (third column). Comparison between the second-order MSM result (dash-dotted) and the reference numerical solution directly obtained from the original Eqs. (2a–d) (solid line for stable solution, dotted line for unstable solution, with circle markers on both types of numerical solutions). Coupled solutions, C+ mode and C− mode, are plotted in blue and red, respectively. The uncoupled solution (U2 mode) is plotted in green with solid and dotted lines denote the stable and unstable solutions, respectively. (Color figure online)

concludes that $\lambda_{2,3}$ are purely imaginary. The coupled solutions C+ and C− are then stable.

Following the same reasoning as in the previous section, the second-order solution can be assessed as a perturbation of the first-order, and one can conclude that for small amplitudes, the coupled backbones will thus be stable. Note that following these branches of the solution to higher amplitudes, then the stability might change, leading to secondary bifurcations and loss of stability of the coupled solutions. This is left for further study and outside the scope of the present analytical development.

### 2.6 Stability of the uncoupled U2 solution

In the case of the uncoupled U2 solution, the situation is more intricate since the modulation Eqs. (10a, 10b), (13) in the polar form lead to a singular Jacobian. In fact, $a_1 = 0$ for the U2-mode, which means that $\theta_1$ and thus $\gamma_p$ are not properly defined. One has then to use a Cartesian form of the modulation equations that is written in "Appendix D". In the case of the U2 solution, the eigenvalues of the Jacobian of the modulation equations read (see Eq. (80)):

$$\lambda_1 = 0, \quad \lambda_{2,3} = \pm\sqrt{-N(a_2, 1)N(a_2, -1)}, \tag{30}$$

where $N(a_2, p) = (2\omega_1 - \omega_2)/2 + p\Gamma_1 a_2 + (\Gamma_3 - \Gamma_6/2)a_2^2$. Notice that the zeros of $N(a_2, p)$ in term of $a_2$ are $\zeta_{2,3}$ introduced in Sect. 2.4 and that $2a_2 N(a_2, p)$ is precisely the numerator of $a_1^2$ in Eq. (16). Consequently, the value $a_2 = \zeta_{2,3}$ makes $\lambda_{2,3} = 0$, which immediately proves that there is a change of stability of the U2-mode at the branching points between the U2-mode and the C+/C− modes, depending on the sign of $2\omega_1 - \omega_2$ and of $p = \pm 1$.

Then, assessing the sign of $N(a_2, p)$ seems difficult in the general case of arbitrary values of $\Gamma_{1,3,6}$ but, as done before, we refer to the first-order MSM solution. In this case, $\Gamma_3 = \Gamma_6 = 0$ and the eigenvalues reads:

$$\lambda_{2,3} = \pm\sqrt{\Gamma_1^2 a_2^2 - \frac{(2\omega_1 - \omega_2)^2}{4}} \tag{31}$$

in which the radicand is negative if $0 < a_2 < |\zeta_0|$ and is positive if $a_2 > |\zeta_0|$, with $\zeta_0$ defined in Eq. (24). Consequently, in the case of the first-order MSM solution, the U2-mode is stable for $a_2$ below the branching point with the coupled mode, and is unstable above. The branching point between the U2 and the C+/C− modes is consequently a supercritical pitchfork bifurcation. In the general case for which $\Gamma_{3,6}$ are non-zero, one can use the perturbative reasoning, based on the fact that the coefficients of the second-order are small and that we are evaluating locally the loss of stability at the branching point (which is for small amplitudes). Then, one can conclude that the above findings are still valid with $\zeta_0$ replaced by $\zeta_{2,3}$ (see Fig. 2).

In the special case without detuning, $\sigma = 0$ ($\omega_2 = 2\omega_1$), Eq. (30) predicts that

$$\lambda_{2,3} = \pm a_2\sqrt{4\Gamma_1^2 - (2\Gamma_3 - \Gamma_6)^2 a_2^2}/2. \tag{32}$$

Using the same reasoning as in Sect. 2.4, the radicand of the square root is positive, showing that the eigenvalue are real for all $a_2 > 0$. Consequently in this case without detuning, the U2-mode branch is fully unstable, which is in agreement with the location of the branch point at $a_2 = 0$.

## 3 Backbone curves, frequency response functions and invariant manifolds

### 3.1 Backbone curves

The aim of this section is to illustrate the previous findings on the topology of the solution branches (backbone curves). A special emphasis is set on showing the changes brought by taking into account the cubic terms in the normal form system (2a-d), as compared to the results given by considering only the quadratic resonant monomials, in order to illustrate the effects of the non-resonant quadratic terms. In all the results shown, the second-order MSM solution is used, either by setting to non-zero values only $g_{12}^1$ and $g_{11}^2$, or by considering all the coefficients appearing in (2a–d). The second-order MSM solution is also compared to a reference numerical solution obtained with a continuation procedure. The continuation of periodic orbits is realized thanks to the harmonic balance method (HBM), and the asymptotic numerical method, as implemented in the open code Manlab, which also computes stability [46–48].

The two selected cases are shown respectively in Figs. 3 and 4, depicting the three backbones of the system analyzed in the previous section, for various values of the parameters. The uncoupled, U2-mode, with $a_1 = 0, a_2 \neq 0$ is shown in green, while the two coupled C+ and C− modes are in blue and red.

Figure 3 shows the special case where only the resonant quadratic monomials have been selected ($g_{12}^1 = g_{11}^2 = 1$), while all other coefficients have been set to zero. The system thus reduces to the one studied in [10], with the distinctive feature that a second-order MSM solution is still at hand. Since no cubic terms are present, the uncoupled backbone degenerates to a straight vertical line. The coupled C+ and C− modes share the properties already underlined in [10, 13]. For a negative detuning, the C− mode emerges at zero amplitude for $\omega_{nl} = 2\omega_1$, while the C+ mode emerges at a non-zero $a_2$ amplitude, at $\omega_{nl} = \omega_2$. The situation is reversed for positive detuning, the C+ mode starting with zero amplitude at $\omega_{nl} = 2\omega_1$ and the C− mode branching from the uncoupled solution with a non-zero amplitude. For a perfectly tuned system, $\sigma = 0$, $\omega_2 = 2\omega_1$ and all branches start at zero amplitude.

The main novelties, as compared to the previous studies, are twofold. First the analysis clearly shows that the non-vanishing branch point is exactly on the uncoupled U2-mode, starting either at amplitude $a_2 = \zeta_3$ for negative detuning, or $a_2 = \zeta_2$ for $\sigma > 0$. Second, since a second-order MSM result is shown here, one can observe that the coupled C+/C− branches show an important curvature in the $(\omega_{nl}, a_2)$ plane, which was not the case in the previously shown results using first-order MSM.

Figure 4 shows the more general case where cubic terms are taken into account in the normal form. More specifically, the values have been set to: $g_{12}^1 = g_{11}^2 = 1$, $g_{11}^1 = g_{22}^1 = g_{12}^2 = g_{22}^2 = 0.5$, and $h_{ijk}^p = 0.1$ for $i$, $j$, $k$, and $p = 1, 2$. As a main consequence, the uncoupled U2 backbone is now curved, due to the presence of the non-vanishing $\Gamma_6$ coefficient, see Eq. (19). With the selected values, $\Gamma_6 < 0$ and consequently, the U2-mode shows a softening

behaviour. Interestingly, and as shown in the previous section, the non-zero branch point of the C+ mode, for a negative detuning, is located at $a_2 = \zeta_3$, exactly on the backbone of the uncoupled solution. The same applies for positive detuning, the C− mode branching from the U2 backbone at amplitude $a_2 = \zeta_2$. Since non-zero cubic terms are now present, the shape of the coupled C+/C− backbones shows a much more important curvature, seen in particular in the plane $(\omega_{nl}, a_1)$ where the branches of C+ solution first increases and then decreases.

The comparison between the second-order MSM and the reference numerical solution shows a very good agreement, even in very adverse conditions as the one shown in Fig. 4. Also, the stability analysis led in the previous section is very well recovered by the numerical solution, validating the perturbative reasoning. In particular, U2-mode is seen to lose stability at the supercritical pitchfork bifurcation point as analyzed, where the coupled solution emerges. Also, the stability of the coupled solution is found to be in line with the analytical results, since stable solutions are retrieved for small amplitudes. Interestingly, the numerical solution shows that the coupled branch can lose stability for higher amplitudes, as expected from the analysis following the remarks at the end of Sect. 2.5. Note that in Figs. 3 and 4, the stability of the analytical solution is not addressed at high amplitudes.

As a conclusion to this section, the numerical simulations shown in Figs. 3 and 4 show that the second-order MSM solution presented in Sect. 2.2 is in excellent agreement with a reference numerical solution, both for the quantitative shape of the backbone curves and their stability. Indeed, some discrepancies between the analytical and numerical solutions are observed, especially the response of the C+ backbone in Fig. 4 d,e,f due to the approximate nature of MSM at high amplitudes that can be corrected by taking into account higher expansion orders.

### 3.2 Forced oscillations: normal form validity and link to the free solutions

This section is devoted to the link between the backbone curves and the forced–damped response of the system, as well as to assess the validity of the normal form transform, Eq. (2), in comparison with the dynamical solutions given by the original equations (1). Since the normal transformation relies on an asymptotic development up to the third order, one needs to assess that the assumption is valid in the range of amplitudes used in the present analysis. In this section, only numerical results will be used, and the second-order MSM solution will not be employed anymore. The numerical solutions are derived thanks to the continuation of periodic orbits with the software Manlab.

The forced–damped frequency response functions will be considered for the original system by adding two linear damping terms $2\xi_1\omega_1\dot{X}_1$ and $2\xi_2\omega_2\dot{X}_2$ to (1a, 1b) where $\xi_1$ and $\xi_2$ are the damping coefficients. The forcing will be considered only on the upper-frequency mode, thus a harmonic force $F\cos\Omega t$ is added to Eq. (1b), where $F$ and $\Omega$ are, respectively, the forcing amplitude and the driving frequency. For the normal form system, Eqs. (6a, 6b) are used, and damping and forcing are added in the same manner. This constitutes an assumption, which holds as long as small values of damping and forcing are considered, which will be the case here. If too large values of the damping are to be considered, then the normal form calculations need to address the damping within the calculations, as shown for example in [23, 37]. Also, for too large values of the forcing, a non-autonomous version of the normal transform must be derived, see for example [49]. For the range of amplitudes investigated in this contribution, the first-order assumption on the damping and forcing is sufficient, and one might consider high-order terms only if larger amplitudes had to be taken into account.

In order to represent the amplitude of the forced–damped solutions, and by analogy with the first-order MSM solution (see e.g. [17]), $X_1(t)$ and $X_2(t)$ are expressed as:

$$X_1(t) = X_{11/2}\cos\left(\frac{\Omega}{2}t - \frac{\gamma_1+\gamma_2}{2}\right) + \text{OH} \tag{33a}$$

$$X_2(t) = X_{21}\cos(\Omega t - \gamma_2) + \text{OH} \tag{33b}$$

where "OH" means other harmonics of smaller amplitude, $\gamma_1$ and $\gamma_2$ are the phase angles and $X_{11/2}$ and $X_{21}$ are respectively the amplitudes of the leading harmonics of $X_1(t)$ and $X_2(t)$. In this solution, $X_2(t)$ is the directly excited degree of freedom that oscillates at the driving frequency $\Omega$ and $X_1(t)$ gains energy through the internal resonance coupling and oscillates

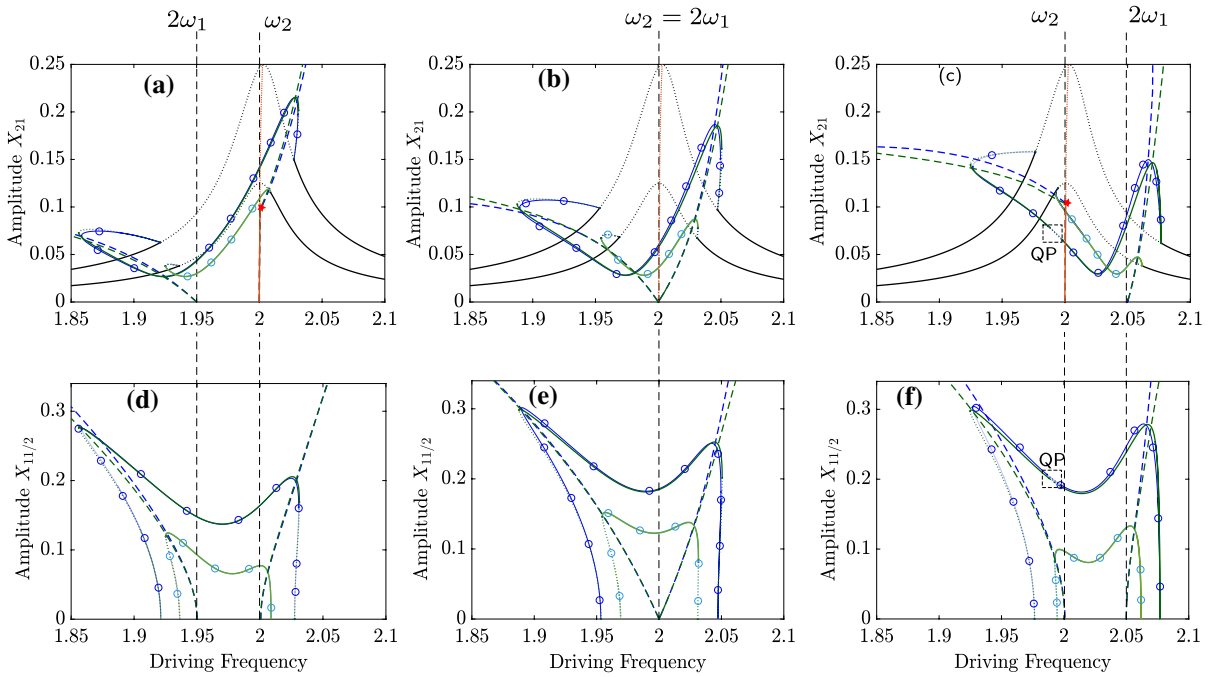


**Fig. 5** Frequency response of the fundamental harmonic amplitude $X_{21}$ of $X_2(t)$ (the first row) and the subharmonic amplitude $X_{11/2}$ of $X_1(t)$ (the second row) for $F = 0.01$ (the lighter color) and $F = 0.02$ (the darker color). The plots are done for $g^1_{11} = g^1_{12} = g^2_{11} = 1$, $g^1_{22} = g^2_{12} = g^2_{22} = 0.03$, all the cubic terms $h^p_{ijk} = 0.3$, $\xi_1 = 0.007$, and $\xi_2 = 0.01$. The first, second, and third column are the results for $\sigma = -0.05$, $\sigma = 0$, and $\sigma = 0.05$, respectively. Comparison between numerical solutions obtained from the original system (blue solid lines with circle markers) and the third-order real normal form (green solid lines). Backbone curves are plotted respectively in blue dashed lines (original system) and green dashed lines (normal form). The uncoupled free and forced solutions are plotted in orange and black, respectively (solid line for stable solutions and dotted lines for unstable). The star symbol denotes the bifurcation point from which coupled solution emerges from the U2 backbone. "QP" denotes the quasi-periodic regime that emerges between two Neimark–Sacker bifurcation points. (Color figure online)

at the subharmonic $\Omega/2$. For the solution obtained from the normal form, Eqs. (6a, 6b), $(R_1(t), R_2(t))$ are back transferred to the physical coordinates $(X_1(t), X_2(t))$ with the nonlinear mapping (3a, 3b), and then the amplitude of the first harmonic is selected for representation.

The comparison between the forced responses of both systems is shown in Fig. 5 for positive, negative, and zero values of $\sigma$. It is observed that the forced solution develops according to the backbone curves of the C+ and C− modes. Namely, the two peaks appearing in the forced response of $X_1$ and $X_2$ lie in the vicinity of the backbone curves. The comparison also shows a very good match between the forced responses of $X_1$ and $X_2$, and the two systems (normal form versus initial system) predict a Neimark–Sacker bifurcation along the coupled branch for $\sigma = 0.05$ leading to quasi-periodic solutions. A small mismatch can be observed at larger amplitudes between the two solutions, and it appears to be more salient on the backbone curves than on the forced-damped solutions, meaning that the validity range of the normal form approximation is more limited in this specific case by the third-order truncation than by the assumptions made on damping and forcing.

A last point worth investigation when comparing free and forced-damped solutions, is the point of coincidence of the two solutions, since it has a significant practical application for observing phase resonance in experiments. A phase resonance occurs when, for a particular driving frequency $\Omega$, the forcing term exactly cancels the damping, such that the oscillator behaves as if it was in undamped free oscillations, see e.g. [50] for a discussion of the general case, [51] for

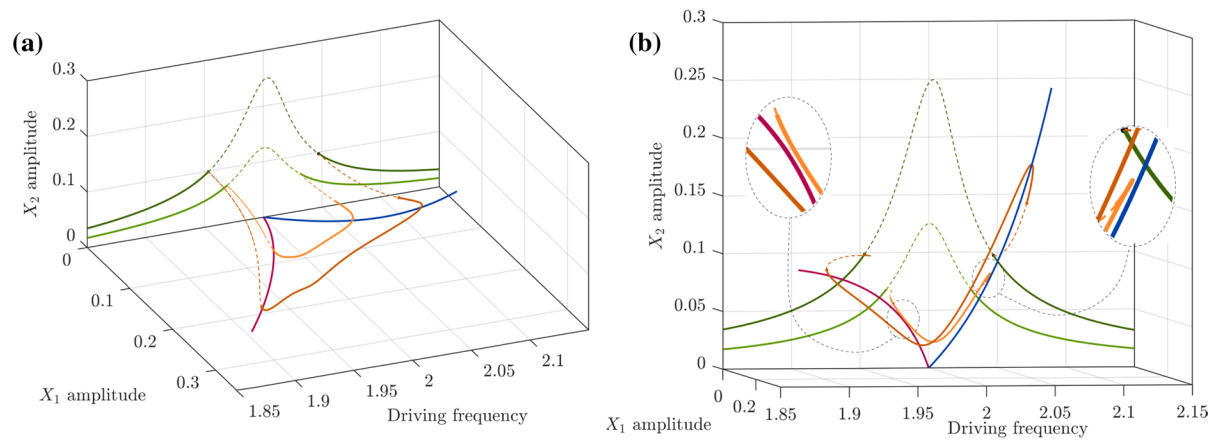


**Fig. 6** Three dimensional view, in the space $(\Omega, X_{11/2}, X_{21})$, of the forced response and the backbone curves, analogous to Fig. 5 with $\sigma = 0$. The uncoupled and coupled forced responses are in green and orange, respectively, whereas the C+ and C− backbone curves are in blue and red, respectively. The unstable parts are shown in dashed lines. (**a**) and (**b**) show different view angles of the same plot to clarify the 3D representation. The zooms are selected to highlight that the free and forced solution branches do not cross each other. (Color figure online)

application to a single DOF problem, and [45] for two cubic oscillators in 1:1 internal resonance.

In the above simulations, since the forcing term is added only to the second oscillator (Eq. 1b), it can only cancel the damping term $2\xi_2\omega_2\dot{X}_2$ of the second oscillator, and not the one of the first oscillator. We then conclude that a phase resonance is not possible here without adding a forcing term also to the first oscillator (Eq. 1a). This is further illustrated with the three-dimensional views of Fig 6, in which one can see in the insets that the forced response *do not intersect* the backbone curves, since they lie in distinct 3D planes. A limit condition for a phase resonance would be to have no damping in the first oscillator ($\xi_1 = 0$). Those results can be verified by comparing Eqs. (33a, 33b) and (17a, 17b), which shows that the phase resonance can be obtained only with $\gamma_1 = k\pi$, which is possible only if $\xi_1 = 0$ and $\gamma_2 = \pi/2$ (see the first-order MSM solution of [17]), the latter result being consistant with a phase resonance of the second oscillator. These results might have very important practical applications if one is interested in applying phase resonance on an experimental system displaying 1:2 internal resonance.

### 3.3 Periodic orbits and 3D manifolds

This section is devoted to illustrating the geometry of the nonlinear modes of the system, viewed as periodic orbits and invariant Lyapunov subcenter manifolds in phase space. The validity limit of the normal form is also addressed by highlighting the departure of the computed manifolds, following the presentation shown in [52].

Families of periodic orbits in the undamped case, following the backbone curves, are numerically computed with the continuation method. Fig. 7 shows the obtained results for the initial system, given by Eqs. (1a, 1b). It can be observed that the C+ and C− modes have similar shapes, up to a change $X_2 \mapsto -X_2$, which is consistent with the parabolic shapes of the periodic orbits in the $(X_1, X_2)$ plane, as shown in Fig. 1. Note that the phase space $(X_1, X_2, \dot{X}_1, \dot{X}_2)$ is four-dimensional, while the manifolds are two-dimensional. In order to represent them, two different projections in three-dimensional spaces are given in Fig. 7a, b, for the perfectly tuned case with $\sigma = 0$. As shown in Sect. 3.1, if $\sigma = 0$, the backbone curves of both C+ and C− modes emerge from zero $X_1 = X_2 = 0$ amplitude, a result consistent with the birth of the manifold at the origin of the phase space in this case. On the other hand, if $\sigma \neq 0$, one of the modes branches from the U2-mode with a pitchfork bifurcation, which corresponds to the black orbit shown in Fig. 7c.

About this branching, a remark is worth to be raised: since the pitchfork is supercritical (see Sects. 2.5 and 2.6), after the bifurcation, two stable

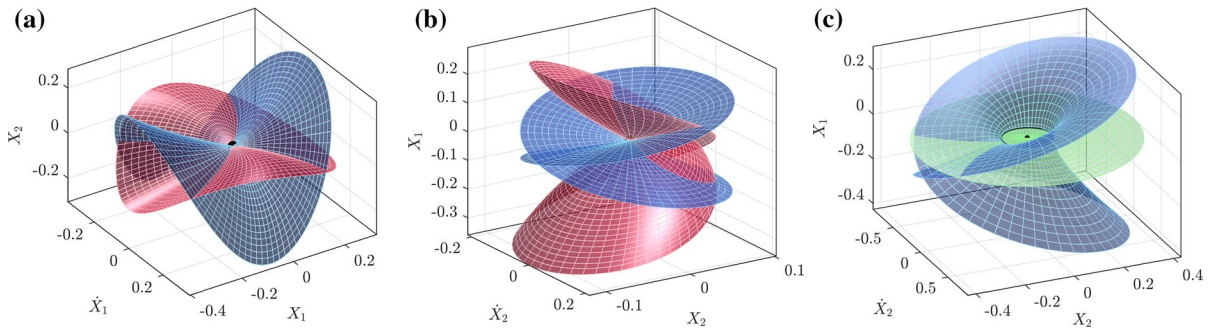


**Fig. 7** Three-dimensional phase space representation of the invariant manifolds (LSM, families of periodic orbits/nonlinear modes) of the initial system given by Eqs. (1a, 1b), computed by numerical continuation. Parameter values selected as in Fig. 5a, b C+ and C− modes, respectively in blue and red, for the perfectly tuned case with $\sigma = 0$ such that $\omega_2 = 2\omega_1$. (**a**) Representation in $(X_1, \dot{X}_1, X_2)$ space, (**b**) in $(X_2, \dot{X}_2, X_1)$ space. (**c**) case with a negative detuning, $\sigma = -0.05$. The manifold in green is the U2-mode (uncoupled solution), which shows a branch point with the C+ mode (in blue). The orbit for which branching is occuring at the pitchfork bifurcation is highlighted in black. A black point shows the origin of the phase space. (Color figure online)

coupled branches are observed. In fact, those two solutions correspond to the two possible values of $k$ for each C+ or C− coupled mode in Eq. (21a). For the C+ mode (resp. the C− mode), $k$ must be even (resp. odd) and $k = 0$ and $k = 2$ (resp. $k = 1$ and $k = 3$) give two different periodic orbits that have the same shape in the phase space (so as the corresponding manifolds), but differ because of a $\pi$ phase shift in $X_1(t)$.

The validity limit of the third-order real normal form approximation can also be ascertained graphically by comparing the invariant manifolds of the initial system, Eq. (1a, 1b), with those obtained with the normal form, as given in Eq. (2). Fig. 8 shows the invariant manifolds of the C+ and C− nonlinear modes computed by numerical continuation with Manlab. On the one hand, the periodic orbits $(X_1(t), X_2(t))$ of the initial system (1a, 1b) are shown in orange color. On the other hand, the third-order normal form of Eq. (2) is used to compute the periodic orbits $(R_1(t), R_2(t))$, which are transformed back to the initial coordinates using the nonlinear mapping (3a, 3b), shown in green. One can observe that the third-order solution suggests an excellent approximation of the reference solution for small amplitudes, consistent with the backbones curves shown in Fig. 5. At higher amplitudes, the third-order manifold departs from the reference solution, in which qualitative changes in the solution are observed. One can note in particular, for the case considered, that the folding of the original manifold shown in Fig. 8d is missed by the third-order approximation. Higher-orders are then needed to recover the folding, as shown for example in [37].

## 4 Recovering the saturation phenomenon

A well-known feature of a system presenting 1:2 resonance is the saturation phenomenon, as recalled in the introduction. This saturation effect is very well described for coupled oscillators including only the resonant quadratic monomials, *i.e.* the terms with coefficients $g^1_{12}$ and $g^2_{11}$ in the initial system (1a, 1b), and gave rise to numerous descriptions and applications in the past, see e.g. [1, 14–16] and references therein. The saturation effect exists when the system is forced in the vicinity of the high-frequency mode $\omega_2$. After a threshold corresponding to the loss of stability of the uncoupled U2-mode, the coupled solution appears, and is characterized by a constant amplitude for $X_2$ when the amplitude of the forcing is increased, meaning that all the energy is transferred to the first oscillator. In terms of the frequency-response functions, this corresponds to the fact that the coupled branch shows a minimum in the vicinity of $\Omega \simeq \omega_2$, which can be interpreted as an anti-resonance. This case is illustrated in Figs. 9a and 10, for the resonant excitation considered in Sect. 3.2, for which the amplitude $X_{21}$ of the H1 harmonics of $X_2(t)$ shows a valley-like shape, with a minimum around

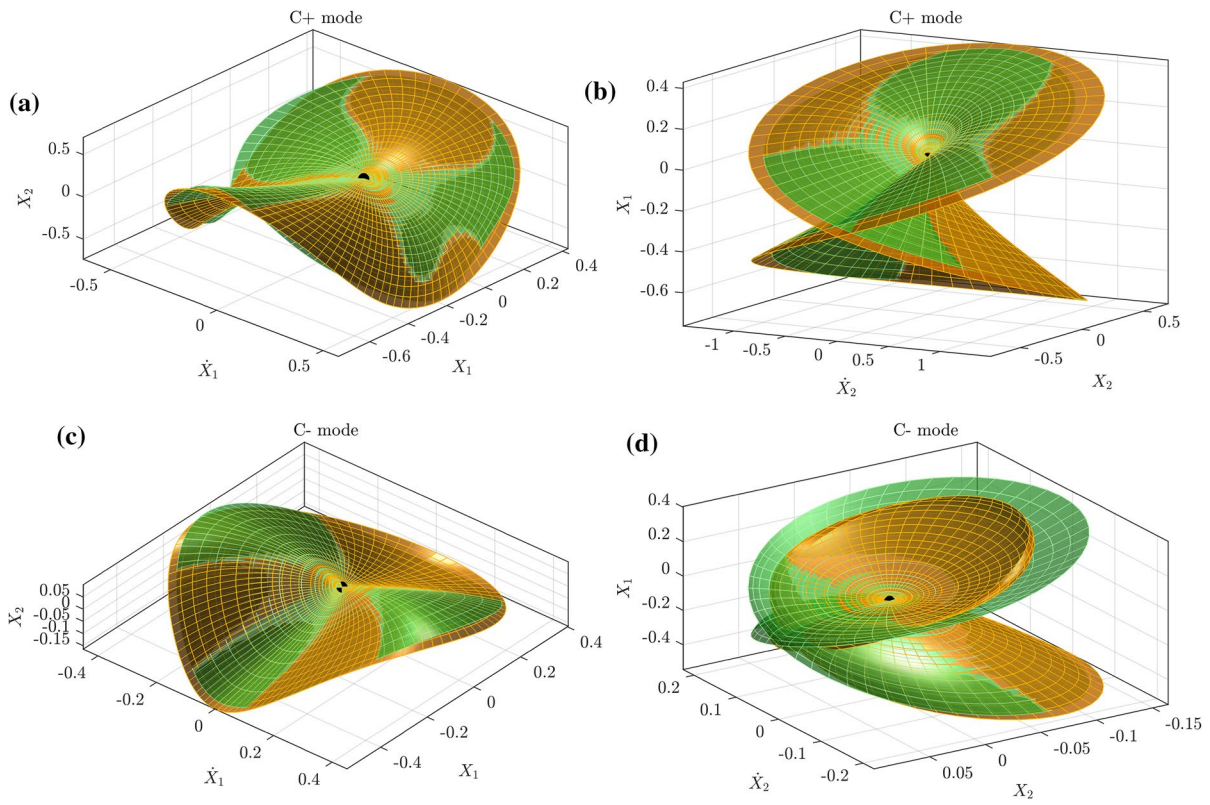


**Fig. 8** Invariant manifolds corresponding to the C+ and C− nonlinear modes of the system, with the parameters of Fig. 5, in the case $\sigma = 0 \Leftrightarrow \omega_2 = 2\omega_1$. Comparison between the numerical solution of the initial system (1a, 1b) (orange, periodic orbits computed with numerical continuation) and the one from the third order normal form of Eq. (2) (green, periodic orbits computed with numerical continuation and back transformed with the nonlinear mapping (3a, 3b)). First row: C+ mode, second row: C− mode. First column, space ($X_1$, $\dot{X}_1$, $X_2$); second column, space ($X_2$, $\dot{X}_2$, $X_1$). The parameters are: $g^1_{11} = g^1_{12} = g^2_{11} = 1$, $g^1_{22} = g^2_{12} = g^2_{22} = 0.03$, and all the cubic terms $h^p_{ijk} = 0.1$. The view angle is different in the first and second row for clarity reason. A black point shows the origin of the phase space. (Color figure online)

$\Omega = \omega_2 = 2$, whose amplitude is almost independent of the forcing ($F$ is multiplied by a factor 3 in the plot). Consequently, locking the frequency of the excitation around the minimum of $X_{21}$ and increasing the amplitude $F$ leads to no increase of $X_{21}$ and thus its saturation.

However, if non-resonant quadratic terms are present in (1a, 1b), it has been observed in [17, 18] that this saturation phenomenon is much less efficient, mainly because the anti-resonance is shifted as the excitation increases. Consequently, if one locks the driving frequency at a given value, then $X_{21}$ at this particular frequency will depend on the driving amplitude $F$, thus severely mitigating the saturation phenomenon. The effect of the non-resonant terms is illustrated in Figs. 9b and 10, with a shift of the anti-resonance toward the low frequencies and a symmetry breaking of the shape of the response curves.

Considering, as explained in Sect. 3.1, that the main effect of both the quadratic non-resonant terms and the cubic ones is to bend the response curves, one could think of using intentionally some cubic terms to *cancel the bending of the response curves* brought by the quadratic terms, using the analytical free solution of the normal form of Sect. 2.2. This idea shares some common points with the one developed in [53], where the nonlinearity is also intentionally tuned in order to create a nonlinear vibration absorber that extends the so-called den Hartog's equal peak method.

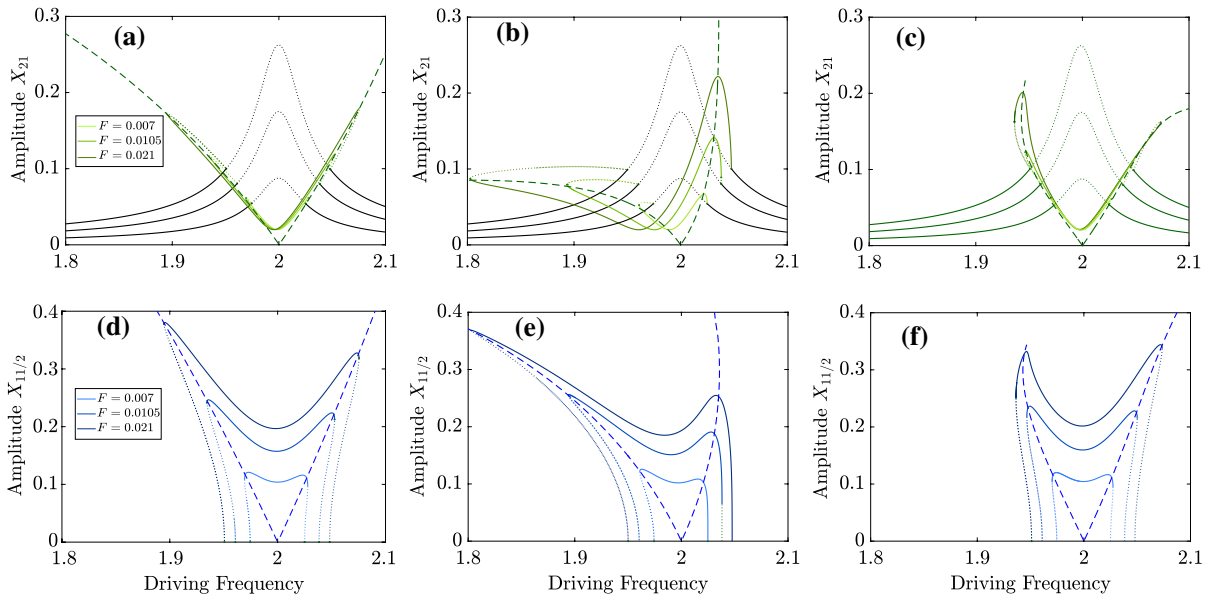


**Fig. 9** Frequency response of the fundamental harmonic amplitude $X_{21}$ of $X_2(t)$ (the first row) and the subharmonic amplitude $X_{11/2}$ of $X_1(t)$ (the second row) for several excitation levels, computed numerically with Manlab in the case $\sigma = 0$ (i.e. $\omega_2 = 2\omega_1$). The first column: only the quadratic resonant terms are considered ($g^1_{12} = g^2_{11} = 1$). The second column: all the quadratic terms are considered with null cubic terms ($g^1_{11} = g^1_{12} = g^2_{11} = 1$, $g^1_{22} = g^2_{12} = g^2_{22} = 0.1$). Third column: all the quadratic terms are considered with the cubic terms are set based on (34a–34d). The damping coefficients are $\xi_1 = 0.007$ and $\xi_2 = 0.01$. The uncoupled forced solution is plotted in black and the coupled solutions are plotted in green and blue. The dotted and solid lines denote the stable and unstable solutions, respectively. The dashed lines denotes the coupled free solution. (Color figure online)

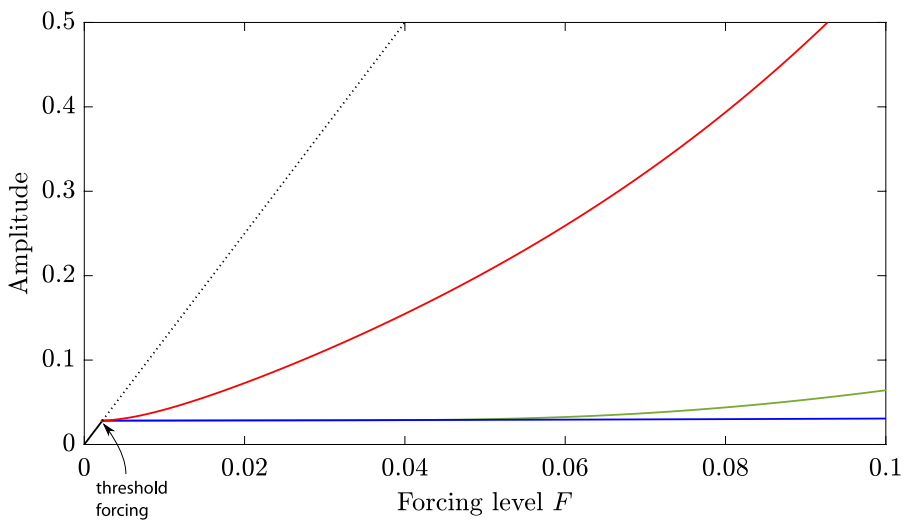


**Fig. 10** Fundamental harmonic amplitude $X_{21}$ of $X_2(t)$ as a function of the excitation level $F$, computed numerically with a continuation method, in the perfectly tuned case $\sigma = 0$ (i.e. $\omega_2 = 2\omega_1$), and for an external excitation frequency $\Omega = \omega_2$, corresponding to the cases of Fig. 9. Black line: linear response with all nonlinear terms cancelled; blue line: only the quadratic resonant terms are considered (Fig. 9a); red line: all the quadratic terms are considered with null cubic terms (Fig. 9b); green line: same quadratic terms with the tuned cubic terms of Eqs. (34a–34d) (Fig. 9c). The solid and dotted lines denote the stable and unstable solutions, respectively. (Color figure online)

In order to do so, the idea is to select the values of the cubic coefficients $h^p_{ijk}$ in order to cancel the effect of the quadratic non resonant terms $g^1_{11}$, $g^1_{22}$, $g^2_{12}$, $g^2_{22}$ in the coefficients $\Gamma_{2,3,5,6}$, such that the backbone curve of Eqs. (18a, 18b) degenerate to those obtained if only the quadratic resonant terms were present. Using the complete expressions of the $\Gamma$ coefficients as reported in the "Appendix C", Eqs. (67b, 67c, 67e, 67f), the following tuning rule expresses the cubic nonlinear coefficients as function of the quadratic non-resonant ones, as:

$$h^1_{111} = \frac{10}{9\omega_1^2}\left(g^1_{11}\right)^2 \tag{34a}$$

$$h^1_{122} = \frac{1}{\omega_2^2}g^1_{12}g^2_{22} - \frac{8\omega_2^2 - 2\omega_1^2}{\omega_1^2(\omega_1^2 - 4\omega_2^2)}g^1_{11}g^1_{22} - \frac{2}{\omega_1^2 - 4\omega_2^2}g^1_{22}g^2_{12} \tag{34b}$$

$$h^2_{112} = \frac{2}{3\omega_2^2}g^2_{11}g^2_{22} + \frac{1}{\omega_1^2}g^1_{11}g^2_{12} - \frac{1}{\omega_1^2 - 4\omega_2^2}\left(g^2_{12}\right)^2 \tag{34c}$$

$$h^2_{222} = \frac{10}{9\omega_2^2}\left(g^2_{22}\right)^2 - \frac{2\omega_2^2 - \omega_1^2}{\omega_1^2(\omega_1^2 - 4\omega_2^2)}g^1_{22}g^2_{12} \tag{34d}$$

Note that only the resonant cubic terms are the parameters to be controlled. The other cubic terms are not considered since they are eliminated in the normal form derivation process, in which it is assumed that such terms have a negligible effect at the third order. To catch the effect of such terms, one has to continue the derivation up to the fourth order, which is not considered in this study.

To validate the proposed technique, Fig. 9c considers the resonant excitation of Sect. 3.2 with the cubic coefficients set as suggested in Eqs. (34a–34d). One observes that this leads first to a lock of the anti-resonance point as the excitation level increases and secondly to response curves with a more symmetric shape, as compared to Fig. 9b where the cubic correction terms are not included. In addition, one can see that for the first two excitation levels, the frequency response is almost identical to that of Fig. 9a, which shows the simplified version of (1a, 1b) where only the quadratic resonant terms are considered. Differences are finally observed when going up to very large amplitudes, which are due to higher-order effects (quintic, ..) that are not taken into account in the analytics. As a final result, Fig. 10 shows that the present tuning of the cubic terms perfectly cancels the effect of the non-resonant quadratic terms, obtaining a perfect saturation phenomenon, up to comfortable amplitudes for an experimental application, and that significantly enhanced the saturation effect obtained by considering only the resonant quadratic terms. In the numerical example considered here, the green and the blue curves almost perfectly match up to an amplitude 23 times the threshold forcing level.

## 5 Conclusion

In this article, the second-order effect of the quadratic non-resonant terms, and the cubic terms, of two oscillators featuring 1:2 internal resonance has been investigated. A special emphasis has been put on the topology of the solution branches for free vibrations (backbone curves) and forced–damped response. The conjugated effect of the non-resonant quadratic terms and the cubic terms, appearing in the same order of expansion in the normal form approach, has been analyzed with a second-order multiple scales expansion. The overall topology in terms of instabilities, bifurcation, and branching is not deeply modified as compared to a first-order analysis; since the most important features of the 1:2 internal resonance are driven by the resonant quadratic terms. However, important quantitative features have been deeply analyzed, complementing already published results on the same problem, which were limited to a first-order development [10, 13].

In the course of the development, numerous interesting results have been derived. The complete analytical derivation of the real normal form for a problem featuring 1:2 internal resonance, and up to the third order, has been shown, complementing the results given in [11, 38] where the assumptions of no internal resonance were retained. The topology of the invariant manifolds linked to the backbone curves/nonlinear modes of the system with 1:2 internal resonance has also been investigated. In particular, the fact that the branch point of the coupled solution is along the uncoupled U2-mode, hence complementing the bifurcation portrait of the conservative problem, has been highlighted. The validity domain of the normal form transform, in both free and forced vibrations, is also assessed by comparisons to numerical

solutions. Finally, the connection between the free and the forced responses of the system has been analyzed, with possible future applications in phase resonance testing of structures with internal resonances [45, 51].

The main application of the analysis presented herein is the improvement of the saturation effect, typical of systems featuring 1:2 internal resonance, and that has already attracted attention in the past in order to design an effective method for passive vibration control. In particular, the simulations show that when the vibration amplitudes increase, cubic nonlinearities cannot be neglected anymore, resulting in numerous effects that have been analyzed with the present developments, in particular the bending of all backbone curves (uncoupled and coupled). Due to the combined effects of quadratic non-resonant and cubic terms, the overall symmetry of the response is broken, the shape of the frequency response curves is importantly modified, and the minimum of the coupled branch, denoted as a sort of anti-resonance, depends strongly on the amplitude, thus destroying the perfectness of the saturation effect. A tuning methodology, involving quadratic non-resonant terms and cubic terms, has thus been proposed in order to recover this saturation effect and enlarge its range of validity, by giving back a more symmetric shape to the frequency response functions.

**Acknowledgements** The Région Hauts de France and the Carnot ARTS Institute, France, are warmly thanked for the PhD grant of the first author.

**Declarations**

**Conflict of interest** The authors declare that they have no conflict of interest.

## A Relationships between nonlinear coefficients

This appendix details the known relationships existing between the coefficients of the monomials given in Eq. (1) when the internal force is assumed to derive from a potential. In such case, the potential energy is a quartic function whose general expression reads:

$$\mathcal{V} = \frac{1}{2}(\omega_1^2 X_1^2 + \omega_2^2 X_2^2) + \frac{1}{3}(g_{11}^1 X_1^3 + g_{22}^2 X_2^3) + g_{11}^2 X_1^2 X_2 + g_{22}^1 X_1 X_2^2 + \frac{1}{4}(h_{111}^1 X_1^4 + h_{222}^2 X_2^4) + \frac{1}{2} h_{112}^2 X_1^2 X_2^2 + h_{111}^2 X_1 X_2^3 + h_{222}^1 X_1^3 X_2. \tag{35}$$

The internal forces are found by deriving this expression with respect to $X_1$ and $X_2$, which leads to the following relationships between the coefficients:

$$g_{12}^1 = 2g_{11}^2, \tag{36a}$$

$$g_{12}^2 = 2g_{22}^1, \tag{36b}$$

$$h_{122}^1 = h_{112}^2, \tag{36c}$$

$$h_{122}^2 = 3h_{222}^1, \tag{36d}$$

$$h_{112}^1 = 3h_{111}^2. \tag{36e}$$

## B Detailed calculation of the normal form

This appendix is devoted to the complete presentation of the calculations needed to arrive at the normal form given in Eq. (2), starting from the original set of two coupled nonlinear oscillators, Eq. (1). The calculation follows the general guidelines given in [11, 38], and is adapted here to take into account the additional condition given by the presence of a 1:2 internal resonance between the two eigenfrequencies of the system. This resonance condition being on the second-order terms will have consequences on the calculation of the cubic terms, which needs to be properly tracked. Since the normal form calculation is sequential in nature, the first step consists in processing the quadratic terms. To that purpose, let us truncate Eq. (1) at the second-order of the nonlinearity, and rewrite them as a first-order problem in time, in order to make clearly appear the contributions due to the two independent variables displacement and velocity:

$$\dot{X}_1 = Y_1, \tag{37a}$$

$$\dot{Y}_1 = -\omega_1^2 X_1 - g_{11}^1 X_1^2 - g_{12}^1 X_1 X_2 - g_{22}^1 X_2^2, \tag{37b}$$

$$\dot{X}_2 = Y_2, \tag{37c}$$

$$\dot{Y}_2 = -\omega_2^2 X_2 - g_{11}^2 X_1^2 - g_{12}^2 X_1 X_2 - g_{22}^2 X_2^2. \tag{37d}$$

A quadratic, indentity-tangent, nonlinear change of coordinates, is first introduced in order to cancel as much as possible the nonlinear terms in Eq. (37). New variables $(U_i, V_i)$ are introduced as:

$$X_1 = U_1 + a^1_{11}U_1^2 + a^1_{12}U_1U_2 + a^1_{22}U_2^2 + b^1_{11}V_1^2 + b^1_{12}V_1V_2 + b^1_{22}V_2^2, \tag{38a}$$

$$Y_1 = V_1 + \gamma^1_{11}U_1V_1 + \gamma^1_{12}U_1V_2 + \gamma^1_{21}U_2V_1 + \gamma^1_{22}U_2V_2, \tag{38b}$$

$$X_2 = U_2 + a^2_{11}U_1^2 + a^2_{12}U_1U_2 + a^2_{22}U_2^2 + b^2_{11}V_1^2 + b^2_{12}V_1V_2 + b^2_{22}V_2^2, \tag{38c}$$

$$Y_2 = V_2 + \gamma^2_{11}U_1V_1 + \gamma^2_{12}U_1V_2 + \gamma^2_{21}U_2V_1 + \gamma^2_{22}U_2V_2. \tag{38d}$$

In these equations, the introduced coefficients $a^p_{ij}$, $b^p_{ij}$, and $\gamma^p_{ij}$, for $i, j, p$=1, 2; are unknowns and will be set according to the idea of canceling non-resonant monomials in the equations of motion. To that purpose, Eq. (38) are differentiated with respect to time and introduced in (37). Identification of the same monomials leads to the values of the coefficients that can be used. Let us first recall the general solution reported in [11, 38] for the case where no internal resonance exists between $\omega_1$ and $\omega_2$. One obtains:

$$\begin{aligned}
&a^1_{11} = \frac{-g^1_{11}}{3\omega_1^2}, \quad b^1_{11} = \frac{-2g^1_{11}}{3\omega_1^4}, \quad \gamma^1_{11} = \frac{2g^1_{11}}{3\omega_1^2}, \quad \gamma^1_{21} = \frac{g^1_{12}}{4\omega_1^2 - \omega_2^2},\\
&a^1_{12} = \frac{g^1_{12}}{\omega_2^2 - 4\omega_1^2}, \quad b^1_{12} = \frac{2g^2_{12}}{\omega_2^2(\omega_2^2 - 4\omega_1^2)}, \quad \gamma^1_{12} = \frac{g^1_{12}(2\omega_1^2 - \omega_2^2)}{\omega_2^2(4\omega_1^2 - \omega_2^2)}, \quad \gamma^2_{21} = \frac{g^2_{12}(\omega_1^2 - 2\omega_2^2)}{\omega_1^2(\omega_1^2 - 4\omega_2^2)},\\
&a^1_{22} = \frac{g^1_{22}(2\omega_2^2 - \omega_1^2)}{\omega_1^2(\omega_1^2 - 4\omega_2^2)}, \quad b^1_{22} = \frac{2g^1_{22}}{\omega_1^2(\omega_1^2 - 4\omega_2^2)}, \quad \gamma^1_{22} = \frac{2g^1_{22}}{4\omega_2^2 - \omega_1^2},\\
&a^2_{11} = \frac{g^2_{11}(\omega_2^2 - 2\omega_1^2)}{\omega_2^2(4\omega_1^2 - \omega_2^2)}, \quad b^2_{11} = \frac{2g^2_{11}}{\omega_2^2(\omega_2^2 - 4\omega_1^2)}, \quad \gamma^2_{11} = \frac{2g^2_{11}}{4\omega_1^2 - \omega_2^2},\\
&a^2_{12} = \frac{g^2_{12}}{\omega_1^2 - 4\omega_2^2}, \quad b^2_{12} = \frac{2g^2_{12}}{\omega_1^2(\omega_1^2 - 4\omega_2^2)}, \quad \gamma^2_{12} = \frac{g^2_{12}}{4\omega_2^2 - \omega_1^2},\\
&a^2_{22} = \frac{-g^2_{22}}{3\omega_2^2}, \quad b^2_{22} = \frac{-2g^2_{22}}{3\omega_2^4}, \quad \gamma^2_{22} = \frac{2g^2_{22}}{3\omega_2^2}.
\end{aligned} \tag{39}$$

In the case of the 1:2 internal resonance condition (i.e., $\omega_2 \approx 2\omega_1$), it appears that the coefficients $a^1_{12}$, $b^1_{12}$, $\gamma^1_{12}$, $\gamma^1_{21}$, $a^2_{11}$, $b^2_{11}$, and $\gamma^2_{11}$ are singular since their denominators contains the term $(\omega_2 - 2\omega_1)$. In such case, the remedy is to set all these coefficients to zero. The coefficients used in Eq. (3) in the main text are thus those given in Eq. (39), except for the singular ones that are replaced by:

$$a^1_{12} = b^1_{12} = \gamma^1_{12} = \gamma^1_{21} = a^2_{11} = b^2_{11} = \gamma^2_{11} = 0. \tag{40}$$

As a consequence, the associated resonant second-order monomials, which are here $g^1_{12}X_1X_2$ and $g^2_{11}X_1^2$, cannot be eliminated from the normal form, in contrary to the other four quadratic terms. After this first step, one is thus able to write the normal form of the problem with 1:2 resonance, up to the quadratic terms, as:

$$\dot{U}_1 = V_1 + O(U_i^3, V_i^3), \tag{41a}$$

$$\dot{V}_1 = -\omega_1^2U_1 - g^1_{12}U_1U_2 + O(U_i^3, V_i^3), \tag{41b}$$

$$\dot{U}_2 = V_2 + O(U_i^3, V_i^3), \tag{41c}$$

$$\dot{V}_2 = -\omega_2^2U_2 - g^2_{11}U_1^2 + O(U_i^3, V_i^3). \tag{41d}$$

The next step of the calculation is to rewrite Eq (41) up to the cubic terms. Besides the original cubic terms with coefficients $h^p_{ijk}$, present in Eq (1), new cubic terms will appear due to the nonlinear nature of the change of coordinates, where products involving linear and quadratic terms will produce new cubic

terms. Let us first focus on the processing of these new terms. In the calculation, the derivatives of Eq. (38) with respect to time need to be computed. The derivative of quadratic terms (e.g. $V_1^2$) makes appear products involving the time derivative ($2V_1\dot{V}_1$ in this case). To eliminate time, one can simply use Eq. (41), such that, up to order four, one can write for the monomial considered as an example: $V_1\dot{V}_1 = -\omega_1^2 U_1 V_1 - g_{12}^1 U_1 U_2 V_1 + O(U_i^4, V_i^4)$, hence making appear the new expected cubic terms. Repeating this procedure for the four equations, and using Eq. (40) to simplify the expressions, one easily arrives at:

$$\dot{U}_1 = V_1 + 2b_{11}^1 g_{12}^1 U_1 U_2 V_1 + 2b_{22}^1 g_{11}^2 U_1^2 V_2, \tag{42a}$$

$$\dot{V}_1 = -\omega_1^2 U_1 - g_{12}^1 U_1 U_2 + \gamma_{11}^1 g_{12}^1 U_1^2 U_2 + \gamma_{22}^1 g_{11}^2 U_1^2 U_2, \tag{42b}$$

$$\dot{U}_2 = V_2 + b_{12}^2 g_{12}^1 U_1 U_2 V_2 + b_{12}^2 g_{11}^2 V_1 U_1^2 + 2b_{22}^2 g_{11}^2 U_1^2 V_2, \tag{42c}$$

$$\dot{V}_2 = -\omega_2^2 U_2 - g_{11}^2 U_1^2 + \gamma_{12}^2 g_{11}^2 U_1^3 + \gamma_{21}^2 g_{12}^1 U_1 U_2^2 + \gamma_{22}^2 g_{11}^2 U_1^2 U_2. \tag{42d}$$

Note that the obtained cubic terms in (42) are solely due to the presence of the 1:2 internal resonance condition. Importantly, those terms were not present in the previous calculations shown in [11, 38], led under the specific assumption of no internal resonance. This means that the general guidelines provided in [11, 38] to derive the normal form can be followed, provided the changes underlined here to take correctly into account a 1:2 resonance.

At this stage, one can observe that the first and third lines, Eqs. (42a)–(42c), are not as simple as they were at the starting point, see e.g. Eq. (37), underlining a simple link between displacement and velocity. To recover this and obtain a more convenient expression of (42a)-(42c), one can define $W_1$ and $W_2$ as:

$$W_1 = V_1 + 2b_{11}^1 g_{12}^1 U_1 U_2 V_1 + 2b_{22}^1 g_{11}^2 U_1^2 V_2, \tag{43a}$$

$$W_2 = V_2 + b_{12}^2 g_{12}^1 U_1 U_2 V_2 + b_{12}^2 g_{11}^2 V_1 U_1^2 + 2b_{22}^2 g_{11}^2 U_1^2 V_2, \tag{43b}$$

such that the system (42) can be rewritten as:

$$\dot{U}_1 = W_1, \tag{44a}$$

$$\begin{aligned}\dot{W}_1 = &-\omega_1^2 U_1 - g_{12}^1 U_1 U_2 + \gamma_{11}^1 g_{12}^1 U_1^2 U_2 \\ &+ \gamma_{22}^1 g_{11}^2 U_1^2 U_2 + 2b_{11}^1 g_{12}^1 (W_1^2 U_2 \\ &+ U_1 W_2 W_1 - U_1^2 U_2 \omega_1^2) + 2b_{22}^1 g_{11}^2 (2U_1 W_1 W_2 - U_1^2 U_2 \omega_2^2) \\ &+ O(U_i^4, W_i^4),\end{aligned} \tag{44b}$$

$$\dot{U}_2 = W_2, \tag{44c}$$

$$\begin{aligned}\dot{W}_2 = &-\omega_2^2 U_2 - g_{11}^2 U_1^2 + \gamma_{12}^2 g_{11}^2 U_1^3 \\ &+ \gamma_{21}^2 g_{12}^1 U_1 U_2^2 + \gamma_{22}^2 g_{11}^2 U_1^2 U_2 \\ &+ b_{12}^2 g_{12}^1 (W_1 U_2 W_2 + U_1 W_2^2 - U_1 U_2^2 \omega_2^2) \\ &+ b_{12}^2 g_{11}^2 (-\omega_1^2 U_1^3 + 2U_1 W_1^2) \\ &+ 2b_{22}^2 g_{11}^2 (2U_1 W_1 W_2 - U_1^2 U_2 \omega_2^2) + O(U_i^4, W_i^4).\end{aligned} \tag{44d}$$

As mentioned earlier, Eq. (44) refer to the problem up to cubic nonlinearity where only the terms added by the presence of the 1:2 resonance have been tracked. We are now in the position of rewriting the complete system up to the third order, on which the next step of the normal transform could be applied by vanishing the non-resonant cubic monomials thanks to a third-order nonlinear change of coordinates. To that purpose, one simply needs to track the cubic terms coming from the original system with $h_{ijk}^p$ coefficients, and those created by the quadratic nonlinear change of coordinate and appearing without the second-order internal resonance. This leads to the following equations:

$$\dot{U}_1 = W_1, \tag{45a}$$

$$\begin{aligned}\dot{W}_1 = &-\omega_1^2 U_1 - g_{12}^1 U_1 U_2 - (h_{111}^1 + A_{111}^1) U_1^3 - (h_{112}^1 + A_{112}^1 - D_{112}^1) U_1^2 U_2 \\ &- (h_{122}^1 + A_{122}^1) U_1 U_2^2 - (h_{222}^1 + A_{222}^1) U_2^3 - B_{111}^1 U_1 W_1^2 - B_{122}^1 U_1 W_2^2 \\ &- (B_{112}^1 - E_{112}^1) U_1 W_1 W_2 - (B_{211}^1 - E_{211}^1) U_2 W_1^2 - B_{212}^1 U_2 W_1 W_2 \\ &- B_{222}^1 U_2 W_2^2 + O(U_i^4, W_i^4),\end{aligned} \tag{45b}$$

$$\dot{U}_2 = W_2, \tag{45c}$$

$$\begin{aligned}\dot{W}_2 = &-\omega_2^2 U_2 - g_{11}^2 U_1^2 - (h_{111}^2 + A_{111}^2 - D_{111}^2)U_1^3 - (h_{112}^2 + A_{112}^2 - D_{112}^2)U_1^2 U_2 \\ &- (h_{122}^2 + A_{122}^2 - D_{122}^2)U_1 U_2^2 - (h_{222}^2 + A_{222}^2)U_2^3 - (B_{111}^2 - E_{111}^2)U_1 W_1^2 \\ &- (B_{122}^2 - E_{122}^2)U_1 W_2^2 - (B_{112}^2 - E_{112}^2)U_1 W_1 W_2 - B_{211}^2 U_2 W_1^2 \\ &- (B_{212}^2 - E_{212}^2)U_2 W_1 W_2 - B_{222}^2 U_2 W_2^2 + O(U_i^4, W_i^4).\end{aligned} \tag{45d}$$

In these equations, the coefficients $A_{ijk}^p$ and $B_{ijk}^p$, with $i,j,k,p = 1,2$; are the same as those already reported in [11, 38], meaning that they arise from the computation of the non internally resonant case. Their general expressions are the same as reported in [11, 38] and read:

$$A_{ijk}^p = \sum_{l\geq i}^{N} g_{il}^p a_{jk}^l + \sum_{l\leq i}^{N} g_{li}^p a_{jk}^l, \tag{46a}$$

$$B_{ijk}^p = \sum_{l\geq i}^{N} g_{il}^p b_{jk}^l + \sum_{l\leq i}^{N} g_{li}^p b_{jk}^l. \tag{46b}$$

As compared to the case without internal resonance, one can note that the general expression is exactly similar, but one has just to take care that due to the 1:2 resonance, some of the $a_{ij}^p$, $b_{ij}^p$, $\gamma_{ij}^p$ coefficients vanish following Eq. (40).

On the other hand, the coefficients $D_{ijk}^p$ and $E_{ijk}^p$, with $i,j,k,p = 1,2$, comes from Eq. (45), and are only due to the presence of the 1:2 internal resonance. They read:

$$\begin{aligned}
D_{112}^1 &= \gamma_{11}^1 g_{12}^1 + \gamma_{22}^1 g_{11}^2 - 2b_{11}^1 g_{12}^1 \omega_1^2 - 2b_{22}^1 g_{11}^2 \omega_2^2, \\
D_{111}^2 &= \gamma_{12}^2 g_{11}^2 - b_{12}^2 g_{11}^2 \omega_1^2, \\
D_{112}^2 &= \gamma_{22}^2 g_{11}^2 - 2b_{22}^2 g_{11}^2 \omega_2^2, \\
D_{122}^2 &= \gamma_{21}^2 g_{12}^1 - b_{12}^2 g_{12}^1 \omega_2^2, \\
E_{112}^1 &= 2b_{11}^1 g_{12}^1 + 4b_{22}^1 g_{11}^2, \\
E_{211}^1 &= 2b_{11}^1 g_{12}^1, \\
E_{111}^2 &= 2b_{12}^2 g_{11}^2, \\
E_{122}^2 &= b_{12}^2 g_{12}^1, \\
E_{112}^2 &= 4b_{22}^2 g_{11}^2, \\
E_{212}^2 &= b_{12}^2 g_{12}^1.
\end{aligned} \tag{47}$$

The last step of the computation of the real normal form up to cubic terms consists of applying a third-order nonlinear change of coordinates in order to cancel all non-resonant cubic monomials in (45). As already noted, for example, in [11, 12, 38], the main difference with second-order is the presence of trivial resonances at the cubic order. Due to the fact that the eigenspectrum is composed of pairs of purely imaginary complex conjugate numbers, trivial resonances are always fulfilled at third order so that numerous monomials cannot be cancelled whatever the values of the eigenvalues. This is in contrast to quadratic terms where, in case of no second-order internal resonance, all the terms can be cancelled by the change of coordinate. Here the procedure simply follows the general guidelines given in [11, 12, 38]. The nonlinear change of coordinates is introduced as:

$$U_p = R_p + \sum_{i=1}^{N}\sum_{j\geq i}^{N}\sum_{k\geq j}^{N} r_{ijk}^p R_i R_j R_k + \sum_{i=1}^{N}\sum_{j=1}^{N}\sum_{k\geq j}^{N} u_{ijk}^p R_i S_j S_k, \tag{48a}$$

$$W_p = \dot{U}_p = S_p + \sum_{i=1}^{N}\sum_{j\geq i}^{N}\sum_{k\geq j}^{N} \mu_{ijk}^p S_i S_j S_k + \sum_{i=1}^{N}\sum_{j=1}^{N}\sum_{k\geq j}^{N} v_{ijk}^p S_i R_j R_k. \tag{48b}$$

To derive the expressions of the unknown coefficients $r_{ijk}^p$, $u_{ijk}^p$, $\mu_{ijk}^p$, and $v_{ijk}^p$, with $i,j,k,p = 1,\ldots,2$; introduced in Eq. (48), one has to differentiate (48) with respect to time and report in the equations of motion, Eq. (45). Identifying the monomials term-by-term leads to explicit expressions for the unknowns, some of them being set directly to zero because of the trivial resonances. Interestingly, this step of the calculation exactly follows the guidelines already provided in [11, 12, 38]. Hence the general formula can be simply used without changes.

After this calculation, most of the cubic monomials present in Eq. (45) can be cancelled by the nonlinear change of coordinates, the only remaining being linked to trivial resonances. Finally, the normal form, up to the third order, and with the 1:2 internal resonance taken into account, reads:

$$\dot{R}_1 = S_1, \tag{49a}$$

$$\dot{S}_1 = -\omega_1^2 R_1 - g_{12}^1 R_1 R_2 - (h_{111}^1 + A_{111}^1) R_1^3 - (h_{122}^1 + A_{122}^1) R_1 R_2^2 - B_{111}^1 R_1 S_1^2 - B_{122}^1 R_1 S_2^2 - B_{212}^1 R_2 S_1 S_2, \tag{49b}$$

$$\dot{R}_2 = S_2, \tag{49c}$$

$$\dot{S}_2 = -\omega_2^2 R_2 - g_{11}^2 R_1^2 - (h_{112}^2 + A_{112}^2 - D_{112}^2) R_1^2 R_2 - (h_{222}^2 + A_{222}^2) R_2^3 - (B_{112}^2 - E_{112}^2) R_1 S_1 S_2 - B_{211}^2 R_2 S_1^2 - B_{222}^2 R_2 S_2^2. \tag{49d}$$

One can note that the normal form is equivalent to that obtained in [11], except for the additional terms $E_{112}^2$ and $D_{112}^2$, which comes as a direct consequence of keeping the resonant quadratic terms due to the 1:2 internal resonance.

## C Detailed calculation of the Multiple scales solution

In this section, we develop the application of the second-order MSM to Eq. (2). The starting point is the system given by Eq. (6), that makes appear the scaled following coefficients:

$$g_{12}^1 = \varepsilon\beta_1, \quad g_{11}^2 = \varepsilon\beta_2, \tag{50a}$$

$$h_{111}^1 + A_{111}^1 = \varepsilon^2\alpha_1, \quad h_{122}^1 + A_{122}^1 = \varepsilon^2\alpha_2, \quad B_{111}^1 = \varepsilon^2\alpha_3, \quad B_{122}^1 = \varepsilon^2\alpha_4, \quad B_{212}^1 = \varepsilon^2\alpha_5, \tag{50b}$$

$$h_{112}^2 + A_{112}^2 - D_{112}^2 = \varepsilon^2\alpha_6, \quad h_{222}^2 + A_{222}^2 = \varepsilon^2\alpha_7, \quad B_{112}^2 - E_{112}^2 = \varepsilon^2\alpha_8, \tag{50c}$$

$$B_{211}^2 = \varepsilon^2\alpha_9, \quad B_{222}^2 = \varepsilon^2\alpha_{10}. \tag{50d}$$

The unknowns $R_1(t)$ and $R_2(t)$ of Eq. (6) are expanded in powers of $\varepsilon$ as:

$$R_1(t;\varepsilon) = r_{10}(T_0,T_1,T_2) + \varepsilon r_{11}(T_0,T_1,T_2) + \varepsilon^2 r_{12}(T_0,T_1,T_2) + O(\varepsilon^3), \tag{51a}$$

$$R_2(t;\varepsilon) = r_{20}(T_0,T_1,T_2) + \varepsilon r_{21}(T_0,T_1,T_2) + \varepsilon^2 r_{22}(T_0,T_1,T_2) + O(\varepsilon^3). \tag{51b}$$

In addition, the first and second derivatives with respect to the initial time $t$ are expressed as:

$$\frac{d}{dt} = D_0 + \varepsilon D_1 + \varepsilon^2 D_2 + O(\varepsilon^3), \tag{52a}$$

$$\frac{d^2}{dt^2} = D_0^2 + 2\varepsilon D_0 D_1 + \varepsilon^2 (D_1^2 + 2D_0 D_2) + O(\varepsilon^3), \tag{52b}$$

where $D_n \equiv \partial/\partial T_n$. Substituting Eq. (51) in (6), using (52) and equating the coefficients of like powers of $\varepsilon$ yields:

- At order $\varepsilon^0$:

$$D_0^2 r_{10} + \omega_1^2 r_{10} = 0, \tag{53a}$$

$$D_0^2 r_{20} + \omega_2^2 r_{20} = 0. \tag{53b}$$

- At order $\varepsilon$:

$$D_0^2 r_{11} + \omega_1^2 r_{11} = -2D_0 D_1 r_{10} - \beta_1 r_{10} r_{20}, \tag{54a}$$

$$D_0^2 r_{21} + \omega_2^2 r_{21} = -2D_0 D_1 r_{20} - \beta_2 r_{10}^2. \tag{54b}$$

- At order $\varepsilon^2$:

$$D_0^2 r_{12} + \omega_1^2 r_{12} = -2D_0 D_1 r_{11} - 2D_0 D_2 r_{10} - D_1^2 r_{10} - \beta_1 r_{10} r_{21} - \beta_2 r_{11} r_{20} - \alpha_1 r_{10}^3 - \alpha_2 r_{10} r_{20}^2 - \alpha_3 r_{10} (D_0 r_{10})^2 - \alpha_4 r_{10} (D_0 r_{20})^2 - \alpha_5 r_{20} D_0 r_{10} D_0 r_{20}, \tag{55a}$$

$$D_0^2 r_{22} + \omega_2^2 r_{22} = -2D_0 D_1 r_{21} - 2D_0 D_2 r_{20} - D_1^2 r_{20} - 2\beta_2 r_{10} r_{11} - \alpha_6 r_{10}^2 r_{20} - \alpha_7 r_{20}^3 - \alpha_8 r_{10} D_0 r_{10} D_0 r_{20} - \alpha_9 r_{20} (D_0 r_{10})^2 - \alpha_{10} r_{20} (D_0 r_{20})^2. \tag{55b}$$

The solutions of (53a, 53b) are expressed as:

$$r_{10} = A_1(T_1, T_2) e^{i\omega_1 T_0} + cc, \tag{56a}$$

$$r_{20} = A_2(T_1, T_2) e^{i\omega_2 T_0} + cc, \tag{56b}$$

where $cc$ stands for the complex conjugate. Upon substituting (56) in (54), the elimination of the resonant terms yield the following solvability condition:

$$D_1 A_1 = \frac{i\beta_1 \bar{A}_1 A_2}{2\omega_1} e^{-i\sigma T_1}, \tag{57a}$$

$$D_1 A_2 = \frac{i\beta_2 A_1^2}{2\omega_2} e^{i\sigma T_1}, \tag{57b}$$

where the internal detuning is $\varepsilon\sigma = 2\omega_1 - \omega_2$, already introduced by Eq. (8) in the main text to quantify the nearness of $\omega_2$ to $2\omega_1$. With the elimination of the resonant terms, Eq. (54) are rewritten as:

$$D_0^2 r_{11} + \omega_1^2 r_{11} = -\beta_1 A_1 A_2 e^{i(\omega_1+\omega_2)T_0} + cc, \tag{58a}$$

$$D_0^2 r_{21} + \omega_2^2 r_{21} = -2\beta_2 A_1 \bar{A}_1. \tag{58b}$$

The solutions of Eq. (58) can be expressed as:

$$r_{11} = B_1 e^{i\omega_1 T_0} + \frac{\beta_1 A_1 A_2}{\omega_2(2\omega_1 + \omega_2)} e^{i(\omega_1+\omega_2)t} + cc, \tag{59a}$$

$$r_{21} = B_2 e^{i\omega_2 T_0} - \frac{\beta_2 A_1 \bar{A}_1}{\omega_2^2} + cc. \tag{59b}$$

Note that in the latter equations, both homogeneous and particular solutions have been taken into account, hence explaining that two terms are present. Indeed, homogeneous solutions to (58) leads to the first terms with coefficients $B_i(T_1, T_2)$, $i = 1, 2$; while the particular solutions give rise to the other two terms.

The modulation equations at order $\varepsilon^2$ can now be constructed by substituting Eqs. (59), (57) and (56) in (55). By canceling the resonant terms, one obtains the solvability condition at this order as:

$$2i\omega_1 D_2 A_1 = \Lambda_1 A_1 A_2 \bar{A}_2 + \Lambda_2 A_1^2 \bar{A}_1 - \sigma \frac{\beta_1 \bar{A}_1 A_2}{2\omega_1} e^{-i\sigma T_1} - \left[ 2i\omega_1 D_1 B_1 + (\beta_1 \bar{A}_1 B_2 + \beta_2 A_2 \bar{B}_1) e^{-i\sigma T_1} \right], \tag{60a}$$

$$2i\omega_2 D_2 A_2 = \Lambda_3 A_1 A_2 \bar{A}_1 + \Lambda_4 A_2^2 \bar{A}_2 + \sigma \frac{\beta_2 A_1^2}{2\omega_2} e^{i\sigma T_1} - \left[ 2i\omega_1 D_1 B_2 + 2\beta_2 A_1 B_1 e^{i\sigma T_1} \right], \tag{60b}$$

with the coefficients $\Lambda_k$ defined in the main text by Eq. (12a–12d).

The present second-order MSM has the peculiarity of the treatment of the homogeneous solution introduced at order $\varepsilon$ (terms of coefficients $B_i$ in Eq. (59)). To derive a solution, one has to find the complex amplitudes $(A_1, A_2, B_1, B_2)$, requiring eight real numbers, whereas the system has two DOFs and thus only four initial conditions. As a consequence, one has to find four real additional relationships to close the problem. In [54, §4.1] and [1, §2.3.1], considering a free Duffing equation, it is shown with a straightforward expansion that it is equivalent to: (i) consider the homogeneous solution of the order $\varepsilon$ system and compute its redundant complex amplitude at the end of the process by considering the initial conditions; and (ii) simply discard the homogeneous solution. In [55, §6.2.1], the MSM, up to second-order, is applied to a Duffing equation using method (ii), since much less algebra is involved. This issue is precisely the subject of [39], in which second-order MSM is applied to several forced one DOFs examples and the free vibration of the 2-DOFs system considered here, Eq. (6), but without cubic terms. It is shown

that better solutions, as compared to those obtained by other perturbation methods, are obtained by considering a non-zero homogeneous solution and by computing it using conditions based on physical considerations. In particular, the system (6) is assumed to derive from a potential energy (with the relations on quadratic and cubic coefficients given in "Appendix A") and the $B_i$ complex amplitudes are selected as functions of $A_i$, such that the modulation equations (60) also derives from a potential. This method is tested in "Appendix E" for our system. However, it seems to us that this approach is not consistent in our case since our initial system (6) does not necessarily derive from a potential. Consequently, as done for the free Duffing equation in [55, §6.2.1], we propose here to simply cancel the homogeneous solution ($B_1 = B_2 = 0$). It is shown in "Appendix E" that the obtained solution is more accurate at large amplitude, compared to a numerical reference simulation. It must also be noted that in [39], a solution with $B_1 = B_2 = 0$ *and* $D_1^2 A_i = 0$ (which leads to cancel also the terms in the second members of Eq. (60) proportional to $\sigma$) is proposed, as well as in [8, 56, 57] for the same system in forced vibrations. Our solution is slightly different as we only enforce $B_1 = B_2 = 0$ and we compute $D_1^2 A_i$ with Eq. (57).

Another issue is the treatment of the two time scales $T_1$ and $T_2$ since our initial ordinary differential equations (ODEs) (6) have been replaced by partial differential equations (57),(60) as functions of the two time scales $(T_1, T_2)$. For simple systems like a free Duffing oscillator, it is possible to exactly integrate them (see [55, §6.2.1]). However, we prefer here recombining them in a single ODE using the chain rule (52a) (also called the reconstitution method [39, 41]), as given by Eq. (9).

The complex-valued amplitudes $A_1(T_1, T_2)$, $A_2(T_1, T_2)$ are expressed in polar form as follows:

$$A_k(T_1, T_2) = \frac{1}{2} a_k(T_1, T_2) e^{i\theta_k(T_1, T_2)}, \quad k = 1, 2. \tag{61}$$

Then, by substituting those equations in Eqs. (57), (60) and by using Eq. (9), the separation of the real and imaginary parts yields to:

$$\dot{a}_1 = \frac{\varepsilon \beta_1 a_1 a_2}{4\omega_1} \left[1 + \frac{\varepsilon\sigma}{2\omega_1}\right] \sin(2\theta_1 - \theta_2 + \sigma T_1), \tag{62a}$$

$$\dot{a}_2 = -\frac{\varepsilon \beta_2 a_1^2}{4\omega_2} \left[1 - \frac{\varepsilon\sigma}{2\omega_2}\right] \sin(2\theta_1 - \theta_2 + \sigma T_1), \tag{62b}$$

$$a_1 \dot{\theta}_1 = \frac{\varepsilon \beta_1 a_1 a_2}{4\omega_1} \left[1 + \frac{\varepsilon\sigma}{2\omega_1}\right] \cos(2\theta_1 - \theta_2 + \sigma T_1) - \varepsilon^2 \frac{\Lambda_1 a_1 a_2^2 + \Lambda_2 a_1^3}{8\omega_1}, \tag{62c}$$

$$a_2 \dot{\theta}_2 = \frac{\varepsilon \beta_2 a_1^2}{4\omega_2} \left[1 - \frac{\varepsilon\sigma}{2\omega_2}\right] \cos(2\theta_1 - \theta_2 + \sigma T_1) - \varepsilon^2 \frac{\Lambda_3 a_1^2 a_2 + \Lambda_4 a_2^3}{8\omega_2}. \tag{62d}$$

It is convenient to rewrite the above equations as:

$$\dot{a}_1 = \Gamma_1 a_1 a_2 \sin\gamma_p, \tag{63a}$$

$$\dot{a}_2 = -\Gamma_4 a_1^2 \sin\gamma_p, \tag{63b}$$

$$a_1 \dot{\theta}_1 = \Gamma_1 a_1 a_2 \cos\gamma_p + \Gamma_2 a_1^3 + \Gamma_3 a_1 a_2^2, \tag{63c}$$

$$a_2 \dot{\theta}_2 = \Gamma_4 a_1^2 \cos\gamma_p + \Gamma_5 a_1^2 a_2 + \Gamma_6 a_2^3. \tag{63d}$$

where

$$\gamma_p = 2\theta_1 - \theta_2 + \sigma T_1, \tag{64}$$

and

$$\Gamma_1 = \frac{\varepsilon\beta_1}{4\omega_1}\left[1 + \frac{\varepsilon\sigma}{2\omega_1}\right], \quad \Gamma_4 = \frac{\varepsilon\beta_2}{4\omega_2}\left[1 - \frac{\varepsilon\sigma}{2\omega_2}\right], \tag{65}$$

$$\Gamma_2 = -\frac{\varepsilon^2\Lambda_2}{8\omega_1}, \quad \Gamma_3 = -\frac{\varepsilon^2\Lambda_1}{8\omega_1}, \quad \Gamma_5 = -\frac{\varepsilon^2\Lambda_3}{8\omega_2}, \quad \Gamma_6 = -\frac{\varepsilon^2\Lambda_4}{8\omega_2}. \tag{66}$$

Those coefficients can be rewritten as function of the initial parameters of the system as

$$\Gamma_1 = \frac{g_{12}^1(4\omega_1 - \omega_2)}{8\omega_1^2}, \tag{67a}$$

$$\Gamma_2 = \frac{1}{8\omega_1}\left[3h_{111}^1 - \left(\frac{2}{\omega_2^2} + \frac{1}{4\omega_1\omega_2}\right)g_{12}^1 g_{11}^2 - \frac{10\left(g_{11}^1\right)^2}{3\omega_1^2}\right], \tag{67b}$$

$$\Gamma_3 = \frac{1}{8\omega_1}\left[2h_{122}^1 + \frac{16\omega_2^2 - 4\omega_1^2}{\omega_1^2(\omega_1^2 - 4\omega_2^2)}g_{11}^1 g_{22}^1 - \frac{2g_{12}^1 g_{22}^2}{\omega_2^2} + \left(\frac{1}{4\omega_1^2} + \frac{1}{\omega_2(2\omega_1 + \omega_2)}\right)\left(g_{12}^1\right)^2 + \frac{4g_{22}^1 g_{12}^2}{\omega_1^2 - 4\omega_2^2}\right], \tag{67c}$$

$$\Gamma_4 = \frac{g_{11}^2(3\omega_2 - 2\omega_1)}{8\omega_2^2}, \tag{67d}$$

$$\Gamma_5 = \frac{1}{8\omega_2}\left[2h_{112}^2 + \frac{2}{\omega_1^2 - 4\omega_2^2}\left(g_{12}^2\right)^2 - \frac{4g_{11}^2 g_{22}^2}{3\omega_2^2} + \left(\frac{2}{\omega_2(2\omega_1 + \omega_2)} - \frac{1}{2\omega_1\omega_2}\right)g_{12}^1 g_{11}^2 - \frac{2g_{11}^1 g_{12}^2}{\omega_1^2}\right], \tag{67e}$$

$$\Gamma_6 = \frac{1}{8\omega_2}\left[3h_{222}^2 + \frac{8\omega_2^2 - 3\omega_1^2}{\omega_1^2(\omega_1^2 - 4\omega_2^2)}g_{22}^1 g_{12}^2 - \frac{10\left(g_{22}^2\right)^2}{3\omega_2^2}\right], \tag{67f}$$

Using Eq. (64) with (63c,d) to eliminate $\theta_1$ or $\theta_2$, one has:

$$\dot{\gamma}_p = 2\omega_1 - \omega_2 + \left(2\Gamma_1 a_2 - \Gamma_4\frac{a_1^2}{a_2}\right)\cos\gamma_p + (2\Gamma_2 - \Gamma_5)a_1^2 + (2\Gamma_3 - \Gamma_6)a_2^2 \tag{68}$$

with

$$J_{13} = \Gamma_1 p a_1 a_2, \quad J_{23} = -\Gamma_4 p a_1^2, \quad J_{31} = -2\Gamma_4 p\frac{a_1}{a_2} + 2(2\Gamma_2 - \Gamma_5)a_1, \quad J_{32} = 2\Gamma_1 p + \frac{\Gamma_4 a_1^2}{a_2^2}p + 2(2\Gamma_3 - \Gamma_6)a_2. \tag{74}$$

## D Stability details

The Jacobian of the modulation equations in polar coordinates (63a, 63b),(68) reads:

$$\boldsymbol{J} = \begin{pmatrix} \Gamma_1 a_2\sin\gamma_p & \Gamma_1 a_1\sin\gamma_p & \Gamma_1 a_1 a_2\cos\gamma_p \\ -2\Gamma_4 a_1\sin\gamma_p & 0 & -\Gamma_4 a_1^2\cos\gamma_p \\ J_{31} & J_{32} & J_{33} \end{pmatrix} \tag{69}$$

with

$$J_{31} = -2\Gamma_4\frac{a_1}{a_2}\cos\gamma_p + 2(2\Gamma_2 - \Gamma_5)a_1, \tag{70}$$

$$J_{32} = \left(2\Gamma_1 + \frac{\Gamma_4 a_1^2}{a_2^2}\right)\cos\gamma_p + 2(2\Gamma_3 - \Gamma_6)a_2, \tag{71}$$

$$J_{33} = -\left(2\Gamma_1 a_2 - \frac{\Gamma_4 a_1^2}{a_2}\right)\sin\gamma_p. \tag{72}$$

For the coupled solutions C+ or C−, $\sin\gamma_p = 0$ and $\cos\gamma_p = p$, which leads to:

$$\boldsymbol{J} = \begin{pmatrix} 0 & 0 & J_{13} \\ 0 & 0 & J_{23} \\ J_{31} & J_{32} & 0 \end{pmatrix} \tag{73}$$

To assess the stability of the uncoupled U2 solution, the modulation equations must be rewritten under a Cartesian form. To do so, according to [4, 31], we define:

$$p_1 = a_1\cos\left(\gamma_p/2\right), \qquad q_1 = a_1\sin\left(\gamma_p/2\right), \qquad p_2 = a_2. \tag{75}$$

Differentiating $p_1$, $q_1$ and $p_2$ with respect to $t$, one obtains:

$$\dot{p}_1 = \dot{a}_1 \cos(\gamma_p/2) - a_1\dot{\gamma}_p/2 \sin(\gamma_p/2), \quad \dot{q}_1 = \dot{a}_1 \sin(\gamma_p/2) + a_1\dot{\gamma}_p/2 \cos(\gamma_p/2), \quad \dot{p}_2 = \dot{a}_2. \tag{76}$$

Then, replacing in the above equations $\dot{a}_1$, $\dot{a}_2$ and $\dot{\gamma}_p$ by their values in the polar modulation equations (63) and (68), using basic trigonometric identities and the definitions (75) of $p_1$, $q_1$ and $p_2$, one replaces the modulation equations (63) and (68) by:

$$\dot{p}_1 = \Gamma_1 p_2 q_1 + \frac{\Gamma_4}{2}\frac{q_1}{p_2}(p_1^2 - q_1^2) - \left(\Gamma_3 - \frac{\Gamma_6}{2}\right)p_2^2 q_1 - \left(\Gamma_2 - \frac{\Gamma_5}{2}\right)q_1(p_1^2 + q_1^2) - \frac{1}{2}(2\omega_1 - \omega_2)q_1, \tag{77a}$$

$$\dot{q}_1 = \Gamma_1 p_1 p_2 - \frac{\Gamma_4}{2}\frac{p_1}{p_2}(p_1^2 - q_1^2) + \left(\Gamma_3 - \frac{\Gamma_6}{2}\right)p_1 p_2^2 + \left(\Gamma_2 - \frac{\Gamma_5}{2}\right)p_1(p_1^2 + q_1^2) + \frac{1}{2}(2\omega_1 - \omega_2)p_1, \tag{77b}$$

$$\dot{p}_2 = -2\Gamma_4 p_1 q_1. \tag{77c}$$

Computing the Jacobian $\boldsymbol{J}$ of the above modulation equations and imposing $a_1 = 0 \Rightarrow p_1 = q_1 = 0$ for the uncoupled U2 solution, one obtains:

$$\boldsymbol{J} = \begin{pmatrix} 0 & J_{12} & 0 \\ J_{21} & 0 & 0 \\ 0 & 0 & 0 \end{pmatrix} \tag{78}$$

with

$$J_{12} = -(2\omega_1 - \omega_2)/2 + \Gamma_1 a_2 - (\Gamma_3 - \Gamma_6/2)a_2^2, \quad J_{21} = (2\omega_1 - \omega_2)/2 + \Gamma_1 a_2 + (\Gamma_3 - \Gamma_6/2)a_2^2, \tag{79}$$

where $a_2 = p_2$ by definition. Its eigenvalues are thus:

$$\lambda_1 = 0, \quad \lambda_{2,3} = \pm\sqrt{J_{12}J_{21}} \tag{80}$$

### E MSM with homogeneous solution and enforced Lagrangian

We consider here the approach of [39] that considers the homogeneous solutions in Eq. (59) and enforces the modulation Eq. (60) to derive from a potential. This is obtained by enforcing:

$$2i\omega_1 D_1 B_1 + D_1^2 A_1 = 0, \quad 2i\omega_1 D_1 B_2 + D_1^2 A_2 = 0, \tag{81}$$

or

$$B_1 = \frac{-\beta_1}{4\omega_1^2} A_2 \bar{A}_1 e^{-i\sigma T_1} + cc, \tag{82a}$$

$$B_2 = \frac{-\beta_2}{4\omega_2^2} A_1^2 e^{i\sigma T_1} + cc. \tag{82b}$$

One can note that upon substituting (82) in (60), all the terms related to $B_1$ and $B_2$ in addition to the terms multiplied by $\sigma$ will be eliminated. We arrive at the following modulation equations:

$$2i\omega_1 D_2 A_1 = \Lambda_1' A_1 A_2 \bar{A}_2 + \Lambda_2' A_1^2 \bar{A}_1, \tag{83a}$$

$$2i\omega_2 D_2 A_2 = \Lambda_3' A_1 A_2 \bar{A}_1 + \Lambda_4' A_2^2 \bar{A}_2, \tag{83b}$$

with

$$\Lambda_1' = \beta_1^2\left[\frac{1}{4\omega_1^2} - \frac{1}{\omega_2(2\omega_1 + \omega_2)}\right] - 2\alpha_4\omega_2^2 - 2\alpha_2, \tag{84a}$$

$$\Lambda_2' = \frac{9\beta_1\beta_2}{4\omega_2^2} - \alpha_3\omega_1^2 - 3\alpha_1, \tag{84b}$$

$$\Lambda_3' = 2\beta_1\beta_2\left[\frac{1}{4\omega_1^2} - \frac{1}{\omega_2(2\omega_1 + \omega_2)}\right] - 2\alpha_6 - 2\alpha_9\omega_1^2, \tag{84c}$$

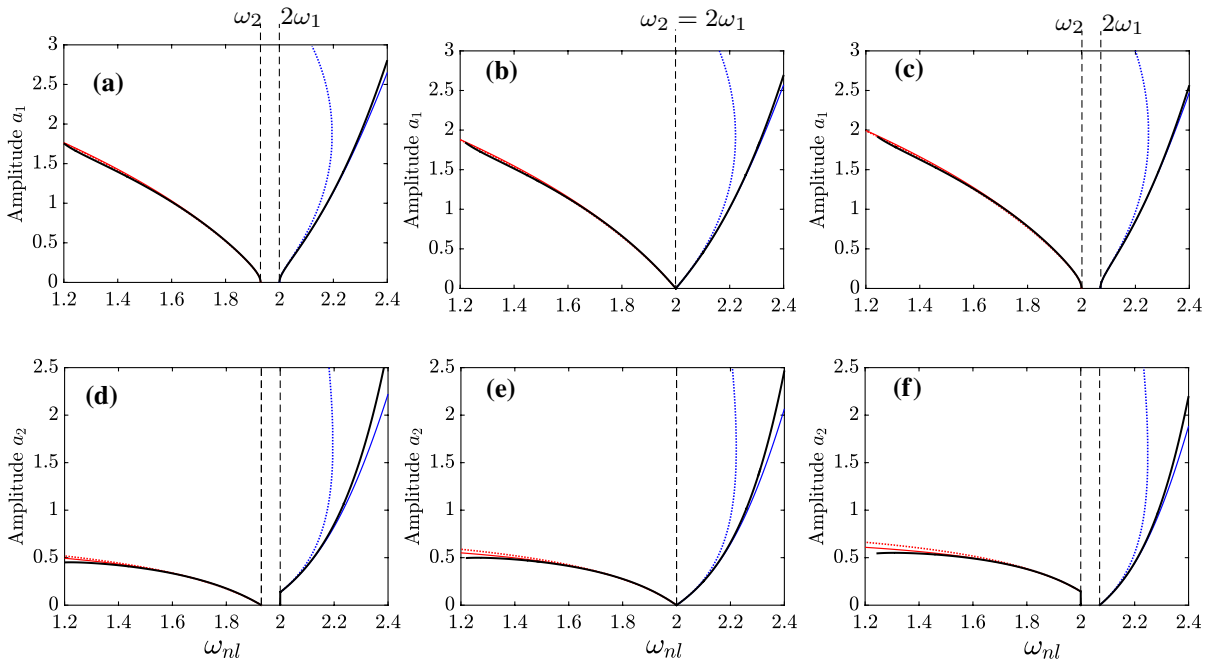


**Fig. 11** Comparison between the analytical results of the two approaches presented in (18a, b) and (87a, b) with the numerical results computed with Manlab. Only the quadratic resonant terms are considered such that $g^1_{12} = g^2_{11} = 1$ with the other nonlinear coefficients are set to zero. The backbones are plotted in the planes ($a_1$, $\omega_{\text{nl2}}$) and ($a_2$, $\omega_{\text{nl2}}$) in the first and second row, respectively. The first, second, and third column are the results for $\sigma = -0.07$, $\sigma = 0$, $\sigma = 0.07$, respectively. The analytical results for the C+ and C− modes are plotted in blue and red, respectively. The dotted and solid lines are results of (87) and (18), respectively. The Manlab results are shown in black for the C+ and C− modes. (Color figure online)

$$\Lambda'_4 = -3\alpha_7 - \alpha_{10}\omega_2^2. \tag{84d}$$

Note that coefficients $\Lambda'_k$ are different than the $\Lambda_k$ in Eq. (60). In addition, one can note that the modulation equations in (83a, b) don't derive from a potential since $\Lambda'_1 \neq \Lambda'_3$ even if it is the case for the initial system (i.e., by setting $g^1_{12} = 2g^2_{11}$, $g^2_{12} = 2g^1_{22}$, $h^1_{122} = h^2_{112}$, $h^2_{122} = 3h^1_{222}$ and $h^1_{112} = 3h^2_{111}$). This can be analyzed by realizing that if one considers the initial system (1a, 1b) to derivee from a potential, it is not necessarily the case for the normal form system (2a, 2b) which relies on a truncation from an asymptotic development. In particular, if one neglects all the cubic terms from ((2a, 2b), one obtains the same results as in [39] where the Lagrangian is enforced.

Following the same procedure in Sect. 2.2, the modulation equations are expressed in the polar form as:

$$\frac{\mathrm{d}a_1}{\mathrm{d}t} = \frac{\varepsilon\beta_1 a_1 a_2}{4\omega_1}\sin\gamma_p, \tag{85a}$$

$$\frac{\mathrm{d}a_2}{\mathrm{d}t} = -\frac{\varepsilon\beta_2 a_1^2}{4\omega_2}\sin\gamma_p, \tag{85b}$$

$$\frac{\mathrm{d}\theta_1}{\mathrm{d}t} = \frac{\varepsilon\beta_1 a_2}{4\omega_1}\cos\gamma_p - \varepsilon^2\frac{\Lambda'_1 a_2^2 + \Lambda'_2 a_1^2}{8\omega_1}, \tag{85c}$$

$$\frac{\mathrm{d}\theta_2}{\mathrm{d}t} = \frac{\varepsilon\beta_2 a_1^2}{4\omega_2 a_2}\cos\gamma_p - \varepsilon^2\frac{\Lambda'_3 a_1^2 + \Lambda'_4 a_2^2}{8\omega_2}, \tag{85d}$$

and the autonomous version is obtained by combining (85c, 85d) with Eq. (11), yielding:

$$\frac{\mathrm{d}\gamma_p}{\mathrm{d}t} = \varepsilon\sigma + \varepsilon\left(\frac{\beta_1 a_2}{2\omega_1} - \frac{\beta_2 a_1^2}{4a_2\omega_2}\right)\cos\gamma_p + \varepsilon^2\left(\frac{\Lambda'_3 a_1^2 + \Lambda'_4 a_2^2}{8\omega_2} - \frac{\Lambda'_1 a_2^2 + \Lambda'_2 a_1^2}{4\omega_1}\right). \tag{86}$$

Using the same procedure in Sect. 2.2, we can find the expressions governing the relation between $a_1$ and $a_2$ in addition to the expressions of the nonlinear modes $\omega_{\mathrm{nl}1}$ and $\omega_{\mathrm{nl}2}$, as:

$$a_1^2 = \frac{(2\omega_1 - \omega_2)a_2 + 2\Gamma'_1 a_2^2 + (2\Gamma'_3 - \Gamma'_6)a_2^3}{\Gamma'_4 + (\Gamma'_5 - 2\Gamma'_2)a_2}, \tag{87a}$$

$$\omega_{\mathrm{nl}1} = \omega_1 + \Gamma'_1 a_2 + \Gamma'_2 a_1^2 + \Gamma'_3 a_2^2, \tag{87b}$$

$$\omega_{\mathrm{nl}2} = \omega_2 + \Gamma'_4 \frac{a_1^2}{a_2} + \Gamma'_5 a_1^2 + \Gamma'_6 a_2^2, \tag{87c}$$

where

$$\Gamma'_1 = p\,\frac{g^1_{12}}{4\omega_1}, \tag{88a}$$

$$\Gamma'_2 = \frac{1}{8\omega_1}\left[3h^1_{111} - \frac{9}{4\omega_2^2}g^1_{12}g^2_{11} - \frac{10}{3\omega_1^2}\left(g^1_{11}\right)^2\right], \tag{88b}$$

$$\Gamma'_3 = \frac{1}{8\omega_1}\left[2h^1_{122} + \left(\frac{16\omega_2^2 - 4\omega_1^2}{\omega_1^2(\omega_1^2 - 4\omega_2^2)}\right)g^1_{11}g^1_{22} - \frac{2g^1_{12}g^2_{22}}{\omega_2^2} + \left(\frac{1}{\omega_2(2\omega_1 + \omega_2)} - \frac{1}{4\omega_1^2}\right)\left(g^1_{12}\right)^2 + \frac{4g^1_{22}g^2_{12}}{\omega_1^2 - 4\omega_2^2}\right], \tag{88c}$$

$$\Gamma'_4 = p\,\frac{g^2_{11}}{4\omega_2}, \tag{88d}$$

$$\Gamma'_5 = \frac{1}{8\omega_2}\left[2h^2_{112} + \left(\frac{2}{\omega_1^2 - 4\omega_2^2}\right)\left(g^2_{12}\right)^2 - \frac{4g^2_{11}g^2_{22}}{3\omega_2^2} + \left(\frac{2}{\omega_2(2\omega_1 - \omega_2)} - \frac{1}{4\omega_1^2}\right)g^1_{12}g^2_{11} - \frac{2g^1_{11}g^2_{12}}{\omega_1^2}\right], \tag{88e}$$

$$\Gamma'_6 = \frac{1}{8\omega_2}\left[3h^2_{222} + \left(\frac{8\omega_2^2 - 3\omega_1^2}{\omega_1^2(\omega_1^2 - 4\omega_2^2)}\right)g^1_{22}g^2_{12} - \frac{10\left(g^2_{22}\right)^2}{3\omega_2^2}\right], \tag{88f}$$

Note that the relation $\omega_{\mathrm{nl}2} = 2\omega_{\mathrm{nl}1}$ is still satisfied. In addition, the solution of $R_1(t)$ and $R_2(t)$ illustrates the same locking properties in the amplitudes and phase angles illustrated in Section 2.2.

A comparison is shown in Fig. 11 between the analytical results governing the backbone curves of both approaches presented in (18a, 18b) and (87b, 87c), with the numerical solution computed with the continuation method implemented in Manlab, which is considered as our reference solution. The plots are done for positive, negative, and zero values of $\sigma$ to underline the effect of the additional term appearing in (60a, 60b). Both results match with the numerical solution at low amplitudes. However, at higher amplitudes, the first approach used in Sect. 2.2 suggests more accurate results as compared to the numerical ones, especially for the C+ mode. Namely, the second approach that leads to the results in (87b, 87c) shows a kind of softening behavior associated with the response of the C+ mode at high amplitudes.

## References


1. Nayfeh A, Mook D (1979) Nonlinear Oscillations, In: Pure and applied mathematics. A Wiley Series of Texts, Monographs and Tracts, Wiley
2. Thomsen JJ (2003) Vibrations and stability. Advanced theory, analysis and tools, 2nd edn. Springer, Berlin, Heidelberg
3. Strogatz S (2014) Nonlinear dynamics and chaos, with applications to physics, biology, chemistry and engineering, 2nd edn. Westview Press, New-York
4. Nayfeh AH (2000) Nonlinear interactions: analytical, computational, and experimental methods. Wiley
5. Nayfeh SA, Nayfeh AH (1993) Nonlinear intercations between two widely spaced modes: external excitation. Int J Bifurc Chaos 3(2):417–427
6. Nayfeh AH, Mook DT, Marshall LR (1973) Nonlinear coupling of pitch and roll modes in ship motions. J Hydronaut 7(4):145–152
7. Miles JW (1984) Resonantly forced motion of two quadratically coupled oscillators. Phys D 13:247–260
8. Lee CL, Perkins NC (1992) Nonlinear oscillations of suspended cables containing a two-to-one internal resonance. Nonlinear Dyn 3:465–490
9. Tien WM, Namachchivaya NS, Bajaj AK (1994) Nonlinear dynamics of a shallow arch under periodic excitation, I : 1:2 internal resonance. Int J Non-linear Mech 29(3):349–366
10. Gobat G, Guillot L, Frangi A, Cochelin B, Touzé C (2021) Backbone curves, Neimark–Sacker boundaries and appearance of quasi-periodicity in nonlinear oscillators: application to 1:2 internal resonance and frequency combs in MEMS. Meccanica 56:1937–1969

11. Touzé C, Thomas O, Chaigne A (2004) Hardening/softening behaviour in non-linear oscillations of structural systems using non-linear normal modes. J Sound Vib 273(1–2):77–101
12. Touzé C (2014) Normal form theory and nonlinear normal modes: theoretical settings and applications. In: Kerschen G (ed) Modal analysis of nonlinear mechanical systems, vol 555. Springer Series CISM courses and lectures, New York, pp 75–160
13. Lenci S, Clementi F, Kloda L, Warminski J, Rega G (2021) Longitudinal-transversal internal resonances in Timoshenko beams with an axial elastic boundary condition. Nonlinear Dyn 103:3489–3513
14. Oueini SS, Nayfeh AH, Pratt JR (1998) A nonlinear vibration absorber for flexible structures. Nonlinear Dyn 15:259–282
15. Pai PF, Rommel B, Schulz MJ (2000) Dynamics regulation of a Skew cantilever plate Using PZT Patches and Saturation Phenomenon. J Intell Mater Syst Struct 11:642–655
16. Wood HG, Roman A, Hanna JA (2018) The saturation bifurcation in coupled oscillators. Phys Lett A 382:1968–1972
17. Shami ZA, Giraud-Audine C, Thomas O (2022) A nonlinear piezoelectric shunt absorber with a 2:1 internal resonance: Theory. Mech Syst Sig Process 170:108768
18. Shami ZA, Giraud-Audine C, Thomas O (2022) A nonlinear piezoelectric shunt absorber with 2:1 internal resonance: experimental proof of concept. Smart Materials and Structures. online
19. Jézéquel L, Lamarque CH (1991) Analysis of non-linear dynamical systems by the normal form theory. J Sound Vib 149(3):429–459
20. Neild SA, Champneys AR, Wagg DJ, Hill TL, Cammarano A (2015) The use of normal forms for analysing nonlinear mechanical vibrations. Proc R Soc A 373:20140404
21. Murdock J (2003) Normal forms and unfoldings for local dynamical systems. Springer Monographs in Mathematics, New-York
22. Kahn PB, Zarmi Y (2014) Nonlinear dynamics: exploration through normal forms. Over Books on Physics
23. Touzé C, Amabili M (2006) Nonlinear normal modes for damped geometrically nonlinear systems: application to reduced-order modelling of harmonically forced structures. J Sound Vib 298:958–981
24. Vizzaccaro A, Shen Y, Salles L, Blahoš J, Touzé C (2021) Direct computation of nonlinear mapping via normal form for reduced-order models of finite element nonlinear structures. Comput Methods Appl Mech Eng 384:113957
25. Opreni A, Vizzaccaro A, Frangi A, Touzé C (2021) Model order reduction based on direct normal form: application to large finite element MEMS structures featuring internal resonance. Nonlinear Dyn 105:1237–1272
26. Haro A, Canadell M, Figueras J-L, Luque A, Mondelo J-M (2016) The parameterization method for invariant manifolds. Springer, From rigorous results to effective computations. Switzerland
27. Touzé C, Vizzaccaro A, Thomas O (2021) Model order reduction methods for geometrically nonlinear structures: a review of nonlinear techniques. Nonlinear Dyn 105:1141–1190
28. Amabili M (2008) Nonlinear vibrations and stability of shells and plates. Cambridge University Press
29. Thomas O, Touzé C, Chaigne A (2005) Non-linear vibrations of free-edge thin spherical shells: modal interaction rules and 1:1:2 internal resonance. Int J Solids Struct 42(11–12):3339–3373
30. Muravyov AA, Rizzi SA (2003) Determination of nonlinear stiffness with application to random vibration of geometrically nonlinear structures. Comput Struct 81(15):1513–1523
31. Pai PF, Wen B, Naser AS, Schultz MJ (1998) Structural vibration control using PZT patches and non-linear phenomena. J Sound Vib 215(2):273–296
32. Leung A, Zhang Q (1998) Complex normal form for strongly non-linear vibration system exemplified by Duffing: van der Pol equation. J Sound Vib 213(5):907–914
33. Elphick C, Iooss G, Tirapegui E (1987) Normal form reduction for time-periodically driven differential equations. Phys Lett A 120(9):459–463
34. Wagg DJ (2022) Normal form transformations for structural dynamics: an introduction for linear and nonlinear systems. J Struct Dyn 1
35. Iooss G, Adelmayer M (1998) Topics in bifurcation theory. World Scientific
36. Neild SA, wagg DJ (2011) Applying the method of normal forms to second-order nonlinear vibration problems. Proc R Soc A 467:1141–1163
37. Vizzaccaro A, Opreni A, Salles L, Frangi A, Touzé C (2021) High order direct parametrisation of invariant manifolds for model order reduction of finite element structures: application to large amplitude vibrations and uncovering of a folding point. Nonlinear Dynamics. submitted
38. Touzé C (2003) A normal form approach for non-linear normal modes, tech. rep., Publications du LMA, numéro 156, (ISSN: 1159-0947, ISBN: 2-909669-20-3)
39. Nayfeh AH (2005) Resolving controversies in the application of the method of multiple scales and the generalized method of averaging. Nonlinear Dyn 40:61–102
40. Clementi F, Lenci S, Rega G (2020) 1:1 internal resonance in a two d.o.f. complete system: A comprehensive analysis and its possible exploitation for design. Meccanica 55:1309–1332
41. Luongo A, Paolone A (1999) On the reconstitution problem in the multiple time-scale method. Nonlinear Dyn 19:133–156
42. Rosenberg RM (1962) The normal modes of nonlinear n-degree-of-freedom systems. J Appl Mech 29:7–14
43. Kerschen G, Peeters M, Golinval JC, Vakakis AF (2009) Non-linear normal modes, part I: a useful framework for the structural dynamicist. Mech Syst Sign rocess 23(1):170–194
44. Manevitch AI, Manevitch LI (2003) Free oscillations in conservative and dissipative symmetric cubic two-degree-of-freedom systems with closed natural frequencies. Meccanica 38(3):335–348
45. Givois A, Tan JJ, Touzé C, Thomas O (2020) Backbone curves of coupled cubic oscillators in one-to-one internal resonance: bifurcation scenario, measurements and parameter identification. Meccanica 55:481–503

46. Guillot L, Lazarus A, Thomas O, Vergez C, Cochelin B (2018) Manlab 4.0: an interactive path-following and bifurcation analysis software. tech. rep., Laboratoire de Mécanique et d'Acoustique, CNRS, http://manlab.lma.cnrs-mrs.fr
47. Guillot L, Cochelin B, Vergez C (2019) A Taylor series-based continuation method for solutions of dynamical systems. Nonlinear Dyn 98:2827–2845
48. Guillot L, Lazarus A, Thomas O, Vergez C, Cochelin B (2020) A purely frequency based Floquet-Hill formulation for the efficient stability computation of periodic solutions of ordinary differential systems. J Comput Phys 416:109477
49. Opreni A, Vizzaccaro A, Touzé C, Frangi A (2022) High order direct parametrisation of invariant manifolds for model order reduction of finite element structures: application to generic forcing terms and parametrically excited systems. Nonlinear Dynamics, submitted
50. Peeters M, Kerschen G, Golinval JC (2011) Dynamic testing of nonlinear vibrating structures using nonlinear normal modes. J Sound Vib 220(3):486–509
51. Denis V, Jossic M, Giraud-Audine C, Chomette B, Renault A, Thomas O (2018) Identification of nonlinear modes using phase-locked-loop experimental continuation and normal form. Mech Syst Sign Process 106:430–452
52. Lamarque C-H, Touzé C, Thomas O (2012) An upper bound for validity limits of asymptotic analytical approaches based on normal form theory. Nonlinear Dyn 70:1931–1949
53. Habib G, Detroux T, Viguié R, Kerschen G (2015) Nonlinear generalization of den Hartog's equal-peak method. Mech Syst Sign Process 52–53:17–28
54. Nayfeh AH (1993) Introduction to perturbation techniques, 1st edn. Wiley Classics Library, Wiley-VCH
55. Nayfeh AH (1973) Perturbation methods. Wiley
56. Benedettini F, Rega G, Alaggio R (1995) Non-linear oscillations of a four-degree-of-freedom model of a suspended cable under multiple internal resonance conditions. J Sound Vib 182(5):775–798
57. Pan R, Davies HG (1996) Responses of a non-linearly coupled pitch-roll ship model under harmonic excitation. Nonlinear Dyn 9:349–368